Reply to the editor's technical corrections

We thank Jan Bottenheim for suggestions regarding technical corrections, which we take into account in the revised manuscript. Comments (in italics) are addressed below. Revised text, where necessary, is shown in blue, and is included in the final manuscript version for ACP. Line numbers refer to the final manuscript (version 2).

I like this paper, too bad it took such a long time to get it to its final stage. I was therefore going to recommend to publish as is to speed this up, but I feel a few corrections and possibly a minor revision are required so I go for publish subject to technical corrections.

Reply: Thank you. We regret as well the delay due to field season commitments as explained to the editorial office.

To start with the need for minor revision: section 3.4 looks to me as quickly put together without proper editing. It is rather sloppily written and contains a couple of rather odd mistakes (see below). Maybe my personal bias but it also has one of the more interesting conclusions: something is missing in the NOx chemistry. The same conclusion is derived from different angles in the paper by Legrand et al, and the recently submitted manuscript by Savarino et al. I for one would emphasize this in the conclusion section but it is so far only mentioned as almost an afterthought. Specific points (numbering refers to the line number in the final manuscript (version 2):

Reply: While we don't find any mistakes in section 3.4, we welcome suggestions to improve the wording (see below). We concur that the conclusions should contain a statement on that the oxidation chemistry at Dome C is not fully understood yet.

Revised text in conclusions; Line 1026: First-time observations of BrO at Dome C suggest that mixing ratios of BrO near the ground are low, certainly less than 5 pptv. Assuming steady-state the observed mixing ratios of BrO and RO_2 radicals are about a factor ten too low to explain the $NO_2 : NO$ ratios measured in ambient air. A potential interference of HO_2NO_2 with the NO_2 measurements explains only a small part of this inconsistency. Hence, the large $NO_2 : NO$ ratios observed at Dome C are either the result of an unknown measurement bias or of a yet unidentified mechanism in boundary layer oxidation chemistry, as similarly concluded in OPALE companion papers (e.g. Legrand et al., 2014; Kukui et al., 2014; Savarino et al., 2015).

194/325: talks about a 4m inlet, but this is never described or referred to (I presume it is more clearly indicated in Frey et al 2013). Please give more info.

Reply: Not really. Sampling heights of 0.01, 1.0 and also that at 4m are indeed mentioned at the very beginning of the method section (Line 151), and results are listed in Table 1, but not specifically discussed in the text, as they did not yield more information over what has been reported in Frey et al. (2013).

Revised text Line 509: In the following we focus on measurements at 0.01 and 1.0m, but statistics from all three measurement heights are reported in Table 1 and 4m measurements were discussed for summer 2009–10 in Frey et al. (2013).

451: I find it odd to call NO3- concentrations in snow an "ancillary measurement", to me it seems to be a key measurement for this paper. I would make it as a separate subchapter, even if the current authors did not make the actual measurements

Reply: Done.

454: "accuracy is larger than usual". I guess it is correct in the sense that accuracy is used here. But at first it gave me the wrong impression that the accuracy was "better" than before. Maybe change it into "the results are less accurate than before".

Reply: Done.

671: section 3.4, as mentioned I recommend to edit the whole section. To me it gives a feeling of handwaiving with numbers.

Reply: Done as shown below and in the revised manuscript.

683: "- the AMFs are incorrect" ?? How so?

Revised text Line 683: this shows that the vertical profile of BrO used to calculate AMFs, whereby all the BrO is in the boundary layer, must be incorrect.

694: "So, if... then..." My first comment would be "yes, but if not... then not..." To me there is very little indication whether the procedure makes sense. I do not suggest to come up with a better one, but formulate it more neutral like "based on the latter observation, we decided to divide the dome-C observations by a factor 3 to arrive at a first estimate of 2-3 pptv"

Revised text Line 694: Based on the similarity of relative changes of slant BrO with elevation angles to those of Halley in 2007, and the approximate ratio of the slant columns at Halley in 2007 to those at Dome C of 3, we decided to divide the Halley inversion results by a factor 3 to arrive at a first estimate for Dome C of 2-3 pptv.

698: "XO = BrO, ClO" Now here is a jump?! If you have ClO data then you better show them. But I suspect this is just a remnant from another manuscript.

Reply: In this expression XO may also be ClO, although not measured. Hence, it is omitted in the revised text.

703-706: again, not wrong, but certainly a rambling sentence.

Revised text Line 194: However, during the same period observations showed a median concentration of $9.9 \times 10^7 \, \mathrm{molecule \, cm^{-3}}$ or $5 \, \mathrm{pptv}$ of $[\mathrm{RO_2}]+[\mathrm{HO_2}]$ (Kukui et al., 2014) and approximately $3 \, \mathrm{pptv}$ of BrO, yielding a total radical concentration $[\mathrm{OX}]$ of $11 \, \mathrm{pptv}$. Hence, $[\mathrm{OX}]$ deduced from measured $NO_2 : NO$ ratios exceeds available observations by a factor 10.3.

715: "9.6 (3.3)". What does the (3.3) refer to? Maybe you mean when 100% of HO2NO2 is interfering? The earlier text makes a case that 25% is the likely factor based on temperature and lifetime in the CLD cell, so why suddenly bringing in the possibility that it should be 100%? Be consistent please.

Reply: Omitted in the revised text.

717: "(not measured)" ? no kidding. This is mentioned far too often, just refer to earlier text where this is discussed, including the likely factor of 25%.

Reply: Done.

1026-1030: conclusion on BrO: firstly saying that "the data suggest 2-3 pptv" is too strong for my taste (these things have a habit of being requoted in future papers and start a life of their own). I would be more comfortable with not quoting numbers but referring to the actual text that it is "probably low, certainly less than 5 pptv".

Reply: We would accept "the data suggest that the mixing ratio of BrO near the ground is low, certainly less than 5 pptv", but "probably" is not appropriate.

Revised text Lines 1026-30: the data suggest that the mixing ratio of BrO near the ground is low, certainly less than 5 pptv.

1026-1030: Furthermore the text with referring to the Theys et al and Salawich et al papers fits more properly in chapter 3.4. And once again, this harping on the potential HO2NO2 interference.... I have not tried to determine how often the potential HO2NO2 interference is referred to, but it sure seems to be invoked frequently. I recommend to skim to manuscript for it and cull the text. After all you talk about a missing measurement that in the end appears not even to be so important anyway.

Reply: The text citing work by Theys et al and Salawich et al is moved to section 3.4. and references to a potential HO2NO2 interference are kept to a minimum.

References

Kukui, A., Legrand, M., Preunkert, S., Frey, M. M., Loisil, R., Gil Roca, J., Jourdain, B., King, M. D., France, J. L., and Ancellet, G.: Measurements of OH and RO_2 radicals at Dome C, East Antarctica, Atmos. Chem. Phys., 14, 12373–12392, doi:10.5194/acp-14-12373-2014, 2014.

Legrand, M., Preunkert, S., Frey, M., Bartels-Rausch, Th., Kukui, A., King, M. D., Savarino, J., Kerbrat, M., and Jourdain, B.: Large mixing ratios of atmospheric nitrous acid (HONO) at Concordia (East Antarctic Plateau) in summer: a strong source from surface snow?, Atmos. Chem. Phys., 14, 9963–9976, doi:10.5194/acp-14-9963-2014, 2014.

Savarino, J., Vicars, W. C., Legrand, M., Preunkert, S., Jourdain, B., Frey, M. M., Kukui, A., Gil and Roca, J.: Oxygen isotope mass balance of atmospheric nitrate at Dome C, East Antarctica, during the OPALE campaign, Atmos. Chem. Phys. Disc., submitted, 2015.

Atmospheric nitrogen oxides (**NO** and **NO$_2$**) at Dome C, East Antarctica, during the OPALE campaign

M. M. Frey[1], H. K. Roscoe[1], A. Kukui[2,3], J. Savarino[4,5], J. L. France[6], M. D. King[6], M. Legrand[4,5], and S. Preunkert[4,5]

[1]British Antarctic Survey, Natural Environment Research Council, Cambridge, UK
[2]Laboratoire Atmosphère, Milieux et Observations Spatiales (LATMOS), UMR8190, CNRS-Université de Versailles Saint Quentin, Université Pierre et Marie Curie, Paris, France
[3]Laboratoire de Physique et Chimie de l'Environnement et de l'Éspace (LPC2E), UMR6115 CNRS-Université d'Orléans, 45071 Orléans cedex 2, France
[4]Université Grenoble Alpes, Laboratoire de Glaciologie et Géophysique de l'Environnement (LGGE), 38000 Grenoble, France
[5]CNRS, Laboratoire de Glaciologie et Géophysique de l'Environnement (LGGE), 38000 Grenoble, France
[6]Department of Earth Sciences, Royal Holloway University of London, Egham, Surrey, TW20 0EX, UK

Correspondence to: M. M. Frey (maey@bas.ac.uk)

Abstract. Mixing ratios of the atmospheric nitrogen oxides NO and NO$_2$ were measured as part of the OPALE (Oxidant Production in Antarctic Lands & Export) campaign at Dome C, East Antarctica (75.1° S, 123.3° E, 3233 m), during December 2011 to January 2012. Profiles of NO$_x$ mixing ratios of the lower 100 m of the atmosphere confirm that, in contrast to South Pole, air chemistry at Dome C is strongly influenced by large diurnal cycles in solar irradiance and a sudden collapse of the atmospheric boundary layer in the early evening. Depth profiles of mixing ratios in firn air suggest that the upper snowpack at Dome C holds a significant reservoir of photolytically produced NO$_2$ and is a sink of gas phase ozone (O$_3$). First-time observations of BrO at Dome C ~~suggest 2–3~~ show that mixing ratios of BrO near the ground are low, certainly less than 5 pptv, with higher levels in the free troposphere. Assuming steady-state, observed mixing ratios of BrO and RO$_2$ radicals are too low to explain the large NO$_2$: NO ratios found in ambient air~~. A possible interference by pernitric acid () may explain part of this inconsistency~~, possibly indicating the existence of an unknown process contributing to the atmospheric chemistry of reactive nitrogen above the Antarctic Plateau. During 2011–2012 NO$_x$ mixing ratios and flux were larger than in 2009–2010 consistent with also larger surface O$_3$ mixing ratios resulting from increased net O$_3$ production. Large NO$_x$ mixing ratios at Dome C arise from a combination of continuous sun light, shallow mixing height and significant NO$_x$ emissions by surface snow ($F_{\mathrm{NO_x}}$). During 23 December 2011–12 January 2012 median $F_{\mathrm{NO_x}}$ was twice that during the same period in 2009–2010 due to significantly larger atmospheric turbulence and a slightly stronger snowpack source. A tripling of $F_{\mathrm{NO_x}}$ in December 2011 was largely due to changes in snow pack source strength caused primarily by changes in NO$_3^-$ concentrations in the snow skin layer, and only to a secondary order by decrease of total column O$_3$ and associated increase in NO$_3^-$ photolysis rates. A source of uncertainty in model estimates of $F_{\mathrm{NO_x}}$ is the quantum yield of ~~nitrate~~ NO$_3^-$ photolysis in natural snow, which may change over time as the snow ages.

1   Introduction

The nitrogen oxides NO and NO_2 ($NO_x = NO + NO_2$) play a key role in the polar troposphere in determining its oxidation capacity, defined here as the sum of O_3, HO_x radicals, and hydrogen peroxide (H_2O_2). The influence is achieved via photolysis of NO_2, the only source for in situ production of tropospheric O_3, through shifting HO_x radical partitioning towards the hydroxyl radical (OH) via the reaction $NO + HO_2 \rightarrow NO_2 + OH$, and finally through reactions with peroxyradicals $NO + HO_2$ (or RO_2) which compete with the formation of peroxides (H_2O_2 and ROOH).

Atmospheric mixing ratios of NO_x in the atmospheric boundary layer of coastal Antarctica are small, with average NO_x values in summer not exceeding 30 pptv (Bauguitte et al., 2012). The build up of large mixing ratios is prevented by gas-phase formation of halogen nitrates (e.g. $BrNO_3$, INO_3) followed by their heterogeneous loss (Bauguitte et al., 2012). Conversely, mixing ratios of NO_x on the East Antarctic Plateau are unusually large, similar to those from the mid-latitudes (Davis et al., 2008; Slusher et al., 2010; Frey et al., 2013). Such large mixing ratios of NO_x were found to arise from a combination of several factors: continuous sunlight, location at the bottom of a large air drainage basin, low temperatures leading to low primary production rates of HO_x radicals, significant emissions of NO_x from surface snow, and a shallow boundary layer (Davis et al., 2008; Frey et al., 2013, and refs. therein).

Snow emissions of NO_x, observed at several polar locations (e.g. Jones et al., 2001; Honrath et al., 2000b), are driven by UV-photolysis of nitrate (NO_3^-) in snow (Honrath et al., 2000b; Simpson et al., 2002) and are now considered to be an essential component of air-snow cycling of oxidised nitrogen species above the polar ice sheets (Davis et al., 2008; Frey et al., 2009b) and likely also above mid-latitude snow packs (Honrath et al., 2000a; Fisher et al., 2005). Atmospheric dynamics, i.e. vertical mixing strength and mixing height, can explain some of the observed temporal variability and site-specific chemical composition of the lower troposphere at South Pole and Summit, Greenland (Neff et al., 2008; Van Dam et al., 2013). Recently, the very strong diurnal cycle of mixing ratios of NO_x observed at Dome C, East Antarctic Plateau, during summer was shown to result from the interplay between boundary layer mixing and emissions from the photochemical snow source; during calm periods a minimum of NO_x mixing ratios occurred around local noon and a maximum in the early evening coinciding with the development and collapse of a convective boundary layer (Frey et al., 2013). A key parameter of the physical atmospheric processes at play is the turbulent diffusivity of the atmosphere, which controls the mixing height, h_z, of the atmospheric boundary layer and contributes to the magnitude of the flux of trace chemical species emitted by the snow (e.g. Frey et al., 2013).

The impact of NO_x emissions from snow on the oxidation capacity of the lower troposphere in summer can be significant. For example, NO_x snow emissions can result in net O_3 production as observed in the interior of Antarctica (Crawford et al., 2001; Legrand et al., 2009; Slusher et al., 2010) as well as unusually large mixing ratios of hydroxyl radicals as detected at South Pole (Davis et al., 2008, and refs. therein). Furthermore, in Antarctica the gas phase production of hydrogen peroxide (H_2O_2), the only major atmospheric oxidant preserved in ice cores, is sensitive to NO released by the surface snowpack (e.g. Frey et al., 2005, 2009a). A steady-state analysis of ratios of $NO_2 : NO$ at Dome C suggested that mixing ratios of peroxy radicals (not measured at the time) are possibly larger at Dome C than any previous observations in air above polar snow (Frey et al., 2013). The quantitative understanding of emissions of NO_x from snow remains incomplete, but it is a research priority to be able to parameterise global models to assess for example global impacts of chemical air-snow exchange on tropospheric O_3 (e.g. Zatko et al., 2013). Emissions of NO_x from snow at Dome C are among the largest observed above either polar ice sheet, but are typically underestimated by models, especially at large solar zenith angles (Frey et al., 2013).

The study presented here was part of the comprehensive atmospheric chemistry campaign OPALE (Oxidant Production and its Export from Antarctic Lands) in East Antarctica (Preunkert et al., 2012) and provided the opportunity to measure NO_x mixing ratios and flux during a second summer season, after a previous campaign in 2009–2010 (Frey et al., 2013). The study objectives were firstly to extend the existing data set with mixing ratio profiles of the lower atmosphere and the firn air (interstitial air) column of the upper snow pack. Secondly, to investigate if observed $NO_2 : NO$ ratios are consistent with measurements of hydroxyl and halogen radicals. And thirdly, to analyse the main drivers of the atmospheric NO_x emission flux from snow.

2   Methods

The measurement campaign of 50 days took place at Dome C ($75.1°$ S, $123.3°$ E, 3233 m) from 23 November 2011 to 12 January 2012. Similar to the 2009–2010 campaign atmospheric sampling was performed from an electrically heated lab shelter (Weatherhaven tent) located in the designated clean-air sector 0.7 km upwind (South) of Concordia station (Frey et al., 2013, Fig.1a). All times are given as local time (LT), equivalent to

UTC + 8 h, and during the study period the sun always remained above the horizon.

2.1 NO_x concentration measurements and uncertainties

Three 20 m-long intake lines (Fluoroline 4200 high purity PFA, I.D. 4.0 mm) were attached to a mast located at 15 m from the lab shelter into the prevailing wind to continuously sample air at 0.01, 1.00 and 4.00 m above the natural snow pack. The intake lines were away from the influence of the drifted snow around the lab shelter. On 9 January 2012 vertical profiles of the lower atmosphere were sampled by attaching a 100 m-long intake line to a helium-filled weather balloon, which was then manually raised and lowered. During selected time periods firn air was sampled, to depths 5–100 cm, by means of a custom built probe. The probe consisted of a tube (10 cm diameter) which was lowered vertically into a pre-cored hole to the chosen snow depth, passing through a disc (1 m diameter) resting on the snow surface. The disk had a lip of 10 cm protruding into the snow. The lip and disk minimised preferential pumping of ambient air along the tube walls. The air intake was mounted so that only air from the bottom and sides could enter, using small horizontal holes at 0-10 cm above the open bottom end of the vertical tube. All probe components were made from UV-transparent plastic (Plexiglas Sunactive GS 2458). Furthermore, 2×3 m sheets of UV-opaque (Acrylite OP-3) and UV-transparent (Acrylite OP-4) plexiglass, mounted on aluminium frames at 1 m above the snow surface, were used to deduce the effect of UV radiation on the mixing ratio of NO_x in the interstitial air and avoid at the same time any temperature effect altering the snow surface.

To measure NO_x the same 2-channel chemiluminescence detector (CLD) and experimental set up as during the 2009–2010 campaign were used (Frey et al., 2013, Fig.1b). Channel one of the CLD measured atmospheric mixing ratios of NO whereas the other channel determined the sum of the mixing ratios of NO and NO originating from the quantitative photolytic conversion of NO_2. The difference between the two channels was used to calculate atmospheric mixing ratios of NO_2. The three sample inlets were connected inside the lab shelter to a valve box, which automatically switched the CLD between sampling heights on a 90 s duty cycle. As described below, the 10-minute average concentration difference ΔNO_x between the 0.01 and 1.0 m inlets is used to estimate flux. Therefore, 10-minute mean ΔNO_x values are calculated on average from two sets of two subsequent 90 s intervals, separated by a 90 s interval during which the 4.0 m inlet was measured. Baseline count rates were determined by adding excess O_3 to sample air in a pre-chamber so that all electronically excited

NO_2 has returned to ground state when reaching the reaction chamber. The baseline was measured for 60 s every 13.5 min alternating between all three inlets. The NO sensitivity of the CLDs was determined every 14 h by standard addition to the sample air matrix of a 1 ppm NO/NO_2 mixture (UK National Physics Laboratory traceable BOC certified), which is further diluted to 4 ppbv of NO. During standard runs also the conversion efficiency (CE) of the photolytic converter was determined by addition of a known mole fraction of NO_2. This was achieved by gas phase titration of the NO/NO_2 mixture to NO_2 by O_3 generated from a pen-ray lamp, and monitoring the un-titrated NO mole fraction. The instrument artefact originating from NO_x producing surface reactions in inlets and reaction cells was determined by overflowing the instrument inlet with scrubbed ambient air supplied by a pure air generator (Eco-Physics PAG003). The artefact was measured every 14 h, offset by 7 h to the calibration runs. The CLD performance, e.g. sensitivity, random error and precision, was similar to that during 2009–10 (Frey et al., 2013, Table 1).

The mean wind direction during the measurement period was from S (176°) with an average speed of $4.0 \, \mathrm{m \, s^{-1}}$ (Fig. 1b). During 2.5% of the time winds came from the direction of Concordia station, i.e. the 355-15° sector (Frey et al., 2013, Fig.1a), potentially carrying polluted air from the station power generator to the measurement site. For example, during Period III. winds rotated 4 times through northerly directions (Fig. 1b). Pollution spikes in the raw 1-s data typically exceeded 10 ppbv of NO_x and were effectively removed before computing the 1-min averages by applying a moving 1-min standard deviation (σ) filter. Observations were rejected when 1-σ of NO and NO_2 mixing ratios within a 1-min window exceeded 24 and 90 pptv, respectively.

The CLD employed also converts nitrous acid (HONO) to NO in the photolytic converter and thus HONO sampled by the CLD is an interferent, as discussed previously (Frey et al., 2013). Average mixing ratios of HONO at 1 m above the snowpack measured with the LOPAP (Long Path Absorption Photometer) technique were ~ 35 pptv (Legrand et al., 2014). The corresponding downward correction for NO_2 at 1 m above the snowpack is $\sim 5\%$. However the LOPAP technique may overestimate the mixing ratio of HONO owing to an interference by pernitric acid (HO_2NO_2) (Legrand et al., 2014). True corrections of NO_2 inferred from modelled HONO mixing ratios (Legrand et al., 2014) are more likely to be on the order of $< 1.5\%$. Due to the uncertainty in absolute mixing ratios of HONO, no correction of NO_x values for the HONO interference was applied.

The thermal decomposition of HO_2NO_2 in the sample lines or photolytic converter of the CLD could also cause a positive bias of NO_x. Spike tests showed that the sample air residence time in the total volume of in-

lets and CLD is $\sim 4\,\mathrm{s}$ (Frey et al., 2013). At a sample flow rate of $5.0\,\mathrm{STP-L\,min^{-1}}$ the residence time in the combined volume of photolytic converter and CLD reaction cell is estimated to be $< 2\,\mathrm{s}$. Atmospheric lifetimes of HO_2NO_2, $\tau_{HO_2NO_2}$, with respect to thermal decomposition to HO_2+NO_2 were calculated at mean ambient pressure ($645\,\mathrm{mb}$) using rate coefficients after Jacobson (1999). $\tau_{HO_2NO_2}$ decreases from $8.6\,\mathrm{h}$ at mean ambient temperature assumed in the sample intake lines ($-30\,^{\circ}\mathrm{C}$) to $7\,\mathrm{s}$ at the maximum observed temperature in the photolytic converter ($30\,^{\circ}\mathrm{C}$). Therefore, NO_2 production from HO_2NO_2 thermal decomposition is negligible in the sample intake lines, but approximately $25\,\%$ of all HO_2NO_2 present may be converted to NO_2 in the photolytic converter. A recent airborne campaign above the East Antarctic Plateau showed mean summertime atmospheric mixing ratios of HO_2NO_2 between 0 and $50\,\mathrm{m}$ of $65\,\mathrm{pptv}$ with maxima about twice as large (Slusher et al., 2010). HO_2NO_2 present at these values could potentially produce 16–$32\,\mathrm{pptv}$ of NO_2 in the photolytic converter equivalent to 8–$16\,\%$ of the average NO_2 mixing ratio measured at $1\,\mathrm{m}$. On 5 January 2012 we attempted to test for the presence of HO_2NO_2 by passing ambient air through a $50\,\mathrm{m}$ intake heated to $50\,^{\circ}\mathrm{C}$ before it entered the CLD. However, during the tests no significant change in NO_2 was detected.

The presence of strong gradients in mixing ratios of HONO inferred by Legrand et al. (2014) can potentially lead to an overestimate of the NO_x concentration differences between 0.01 and $1.0\,\mathrm{m}$ used below to derive the vertical NO_x flux. During the OPALE campaign the atmospheric life time of NO_x, τ_{NO_x}, ranged between $3\,\mathrm{h}$ (12:00 LT) and $7\,\mathrm{h}$ (00:00 LT), whereas that of HONO, τ_{HONO}, ranged between $4.5\,\mathrm{min}$ (12:00 LT) and $24\,\mathrm{min}$ (00:00 LT) (Legrand et al., 2014). The life time of HONO is comparable to the typical transport times of $\sim 10\,\mathrm{min}$ between the surface and $1\,\mathrm{m}$ at Dome C in summer (Frey et al., 2013). Hence, HONO : NO_x ratios as well as corresponding corrections required for NO_2 are not constant with height above the snow surface. No gradients of HONO mixing ratios were measured but modelled values were 18.8 and $10.2\,\mathrm{pptv}$ at noon, and 15.3 and $12\,\mathrm{pptv}$ at midnight, at 0.1 and $1.0\,\mathrm{m}$, respectively (Legrand et al., 2014). Corresponding corrections of mean NO_2 mixing ratios for HONO are 1.3–$1.5\,\%$ with a maximum difference of $0.2\,\%$ between 0.1 and $1.0\,\mathrm{m}$. Thus, at Dome C a strong gradient in the mixing ratios of HONO was a negligible effect on the mixing ratios of NO_x measured at 0.1 and $1.0\,\mathrm{m}$ and thus a negligible effect on the estimated NO_x flux.

2.2 NO_x flux estimates

The turbulent flux of NO_x, F_{NO_x}, was estimated using the integrated flux gradient method (e.g. Lenschow,

1995) and mixing ratios of NO_x measured at 0.01 and $1.0\,\mathrm{m}$. F_{NO_x} in the surface layer is parameterised according to the Monin–Obukhov similarity theory (MOST) whose predictions of flux-profile relationships at Halley, an Antarctic coastal site of the same latitude as Dome C, agree well with observations (Anderson and Neff, 2008, and references therein):

$$F_{NO_x} = -\frac{\kappa u_* z}{\Phi_h\left(\frac{z}{L}\right)}\frac{\partial c}{\partial z} \tag{1}$$

with the von Karman constant κ (set to 0.40), friction velocity u_*, measurement height z, concentration gradient $\partial c/\partial z$, and $\Phi_h\left(\frac{z}{L}\right)$ an empirically determined stability function for heat with L as the Monin–Obukhov length. Assuming constant flux across the layer between the two measurement heights z_1 and z_2 allows the integration to be solved and yields:

$$F_{NO_x} = -\frac{\int_{c_1}^{c_2}\kappa u_*\partial c}{\int_{z_1}^{z_2}\Phi_h\left(\frac{z}{L}\right)\frac{\partial z}{z}} = -\frac{\kappa u_*[c(z_2)-c(z_1)]}{\int_{z_1}^{z_2}\Phi_h\left(\frac{z}{L}\right)\frac{\partial z}{z}} \tag{2}$$

Stability functions Φ_h used are given in Frey et al. (2013), while their integrated forms can be found in Jacobson (1999). Friction velocity u_* and L were computed from the three-dimensional wind components (u, v, w) and temperature measured at $25\,\mathrm{Hz}$ by a sonic anemometer (Metek USA-1) mounted next to the uppermost NO_x intake line, at $4\,\mathrm{m}$ above the snow surface. Processing of raw sonic data in $10\,\mathrm{min}$ blocks included temperature cross-wind correction and a double coordinate rotation to force mean w to zero (Kaimal and Finnigan, 1994; Van Dijk et al., 2006). Equation (2) implies that a positive flux is in upward direction, equivalent to snow pack emissions and a negative flux is in downward direction, equivalent to deposition.

The application of MOST requires the following conditions to be met: (a) flux is constant between measurement heights z_1 and z_2, (b) the lower inlet height z_1 is well above the aerodynamic roughness length of the surface, (c) the upper inlet height z_2 is within the surface layer, i.e. below $10\,\%$ of the boundary layer height h_z (Stull, 1988), and (d) z_1 and z_2 are far enough apart to allow for detection of a significant concentration difference $[c(z_2)-c(z_1)]$.

Condition (a) is met in the surface layer if the chemical lifetime τ_{chem} of NO_x is much longer than the turbulent transport time scale τ_{trans}. Based on observed OH and HO_2 the τ_{chem} for NO_x is estimated to be $3\,\mathrm{h}$ at 1200 LT and $7\,\mathrm{h}$ at 0000 LT during OPALE (Legrand et al., 2014). Estimating τ_{trans} following the approach described previously (Frey et al., 2013, Eq. 6 and 7) yields 0.6, 1.7 and $2.5\,\mathrm{min}$ during the day (0900-1700 LT), the typical time of BL collapse (1700-1900 LT) and during the night (1900-0900 LT), respectively. Thus,

τ_{chem} exceeds τ_{trans} by at least a factor 100, confirming that vertical mixing always dominates over the gas phase photochemical sink and flux can be assumed constant between the two inlets. Condition (b) is met as discussed in Frey et al. (2013). For (c) the upper inlet height of 1 m is compared to estimates of mixing height h_z from the MAR model (Gallée et al., 2015). The MAR model has been validated previously over the Antarctic Plateau, focusing on Dome C, during winter (Gallée and Gorodetskaya, 2010) and now also during summer (Gallée et al., 2015). Calculated flux values of NO_x were removed when $h_z < 10$ m resulting in the removal of 22 % (773 values) of all available 10 min flux averages. Flux estimates are removed specifically during the evening and night, when the BL is shallow. Hence, fluxes during night time are less well constrained, but nevertheless support a significant diurnal cycle (Frey et al., 2013, Fig. 6b,g and Fig. 9). For (d) 10 min averages of $[c(z_2) - c(z_1)]$ not significantly different from zero, i.e. smaller than their respective 1-σ standard error, were not included in the calculation of the flux of NO_x. The 1-σ standard error in $[c(z_2) - c(z_1)]$ was determined by error propagation of the 1-σ standard error of NO_x mixing ratios. A total of 8 % (303 values) of all available 10 min flux averages were not significantly different from zero and thus removed.

In summary, the restrictions imposed by MOST and NO_x measurement uncertainty justify placing inlets at 0.01 and 1.0 m and lead to the removal of 30 % (1076 values) of all available flux estimates. The total uncertainty of the 10 min NO_x flux values due to random error in $[c(z_2) - c(z_1)]$ (31 %), u_* (3 % after Bauguitte et al., 2012) and measurement height (error in $\ln(z_2/z_1)$ of ~ 7 %) amounts to 32 %.

2.3 Analysis of NO_3^- concentrations in snow

During this study NO_3^- concentrations in snow were measured every 2–3 days in the surface skin layer, i.e. in the top 0.5 cm of the snowpack, as well as in shallow snow pits within the clean-air sector. Snow NO_3^- concentrations were determined using clean sampling procedures and a continuous flow analysis technique (e.g. Frey et al., 2009b). Samples were stored together with the additional snow samples discussed in Berhanu et al. (2014) and then analysed for NO_3^- in batches by the same operator. The precision is 5% based on replicate standard measurements. Due to a systematic shift in the NO_3^- standard response in between individual batch runs due to a calibration issue (Berhanu et al., 2014) results are less accurate than before. The overall accuracy including systematic errors in calibration and collection of just the top few mm of snow is of the order of 20%, and is therefore comparable to the spatial variability of NO_3^- in surface snow at Dome C (France et al., 2011). For the discussion below it should be borne in mind that temporal changes of NO_3^- concentrations observed in surface snow are >50% (Fig. 7b) and therefore significantly larger than the measurement accuracy.

2.4 MAX-DOAS observations

Scattered sunlight was observed by a ground-based UV-visible spectrometer, in order to retrieve bromine oxide (BrO) column amounts. The instrument was contained in a small temperature-controlled box, which was mounted onto a tripod at 1 m above the snow surface. An external gearbox and motor scanned the box in elevation (so-called Multiple Axis). Spectra were analysed by Differential Optical Absorption Spectroscopy (DOAS), the combination being known as the MAX-DOAS technique. See Roscoe et al. (2014) for more details of apparatus and analysis. Briefly, the observed spectrum contains Fraunhofer lines from the Sun's atmosphere, which interfere with absorption lines in the Earth's atmosphere and are removed by dividing by a reference spectrum. The amounts of absorbers in the Earth's atmosphere are found by fitting laboratory cross-sections to the ratio of observed to reference spectra, after applying a high-pass filter in wavelength (the DOAS technique).

In our case the spectral fit was from 341 to 356 nm, and the interfering gases O_3, O_4 (oxygen dimer) and NO_2 were included with BrO. The analysis was done with two reference spectra, one from near the start of the campaign in December, the other following the addition of a snow excluder in January, necessary because it also contained a blue glass filter with very different spectral shape. The analysis was restricted to cloud-free days or part-days. In MAX-DOAS geometry, the stratospheric light path is almost identical in low-elevation and zenith views, so stratospheric absorption is removed by subtracting simultaneous zenith amounts from low-elevation slant amounts, important for BrO as there is much in the stratosphere.

To find the vertical amounts of BrO radicals the MAX-DOAS measurements were evaluated as follows: we divided by the ratio of the slant path length to the vertical (the Air Mass Factor, AMF), calculated by radiative transfer code (Mayer and Kylling, 2005), assuming all the BrO was in the lowest 200 m.

2.5 Ancillary measurements and data

Other co-located atmospheric measurements included mixing ratios of OH radicals and the sum of peroxy radicals (RO_2) at 3 m using chemical ionisation mass spectrometry (Kukui et al., 2014) and mixing ratios of

O_3 at 1 m with a UV absorption monitor (Thermo Electron Corporation model 49I, Franklin, Massachusetts). Photolysis rate coefficients, J, were determined based on actinic flux, I, measured at ~ 3.50 m above the snow surface using a Met-Con 2π spectral radiometer equipped with a CCD detector and a spectral range from 285 to 700 nm (further details in Kukui et al., 2014). Total column O_3 above Dome C was taken from ground based SAOZ (Système d'Analyse par Observation Zenitale) observations (http://saoz.obs.uvsq.fr/SAOZ_consol_v2.html). Standard meteorology was available from an automatic weather station (AWS) at 0.5 km distance and included air temperature (Vaisala PT100 DTS12 at 1.6 m), relative humidity (at 1.6 m), wind speed and direction (Vaisala WAA 15A at 3.3 m). The mixing height h_z of the atmospheric boundary layer was calculated from simulations with the MAR model as the height where the turbulent kinetic energy decreases below 5 % of the value of the lowest layer of the model (Gallée et al., 2015).

~~During this study concentrations in snow were measured every 2–3 days in the surface skin layer, i.e. in the top 0.5 of the snowpack, as well as in shallow snow pits within the clean-air sector. Snow concentrations were determined using clean sampling procedures and a continuous flow analysis technique (e.g. Frey et al., 2009b). Samples were stored together with the additional snow samples discussed in Berhanu et al. (2014) and then analysed for in batches by the same operator. The precision is 5% based on replicate standard measurements. Due to a systematic shift in the standard response in between individual batch runs due to a calibration issue (Berhanu et al., 2014) the accuracy is larger than usual. The overall accuracy including systematic errors in calibration and collection of just the top few mm of snow is of the order of 20%, and is therefore comparable to the spatial variability of in surface snow at Dome C (France et al., 2011). For the discussion below it should be borne in mind that temporal changes of concentrations observed in surface snow are >50% (Fig. 7b) and therefore significantly larger than the measurement accuracy.~~

2.6 Modelling NO_3^- photolysis

The flux of NO_2, F_{NO_2}, from the snowpack owing to photolysis of the NO_3^- anion in the snowpack can be estimated as the depth-integrated photolysis rate of NO_3^-

$$F_{NO_2} = \int_{z=0\,m}^{z=1\,m} [NO_3^-]_z \, J_z(NO_3^-) \, dz \qquad (3)$$

where $J_z(NO_3^-)$ is the photolysis rate coefficient of reaction $NO_3^- + h\nu \rightarrow NO_2 + O^-$ at depth, z, in the snowpack. $[NO_3^-]_z$ is the amount of NO_3^- per unit volume of snow at depth, z, in the snowpack. $J_z(NO_3^-)$ is calculated as described in France et al. (2010) using a radiative transfer model, TUV-snow (Lee-Taylor and Madronich, 2002), to calculate irradiances within the snowpack as a function of depth. The optical properties and detailed description of the Dome C snowpack are reported in France et al. (2011). Values of depth-integrated flux were calculated as a function of solar zenith angle and scaled by values of $J(NO_3^-)$ measured by the Met-Con 2π spectral radiometer described above to account for changing sky conditions. Scaling by a measured value of $J(NO_3^-)$ is more accurate than previous efforts of scaling with a broad band UV instrument (e.g. France et al., 2011). The quantum yield and the absorption spectrum for NO_3^- photolysis in snow were taken from Chu and Anastasio (2003). For the discussion below it should be borne in mind that the calculated F_{NO_2} is a potential emission flux assuming that NO_2 is vented immediately after release from the snow grain to the air above the snow pack without undergoing any secondary reactions.

3 Results and discussion

3.1 NO_x observations in ambient and firn air

In summer 2011–2012 atmospheric mixing ratios of NO_x with strong diurnal variability were observed (Fig. 1c), similar to the 2009–2010 season, and showed maximum median levels in firn air of ~ 3837 pptv, which rapidly decreased to 319 pptv at 0.01 m and 213 pptv at 1.0 m (Table 1). In the following we focus on measurements at 0.01 and 1.0 m, but statistics from all three measurement heights are reported in Table 1 and 4 m measurements were discussed for summer 2009–10 in Frey et al. (2013).

As seen previously at Dome C and other locations, NO_x mixing ratios were weakly but significantly anti-correlated with wind speed (at 1.0 m $R = -0.37$, $p < 0.001$), especially when only the time period of the daily collapse of the convective boundary layer, i.e. 1700-1900 LT, was considered ($R = -0.45$, $p < 0.001$), and their diurnal cycle was dampened during storms (Fig. 1b–c).

The two main differences between summer 2011–2012 and summer 2009–2010 are a strong intra-seasonal variability and larger atmospheric mixing ratios. A significant increase of NO_x mixing ratios at 1.0 m from low values in Period I. (23–30 November 2011) occurred in two steps: a small rise in Period II. (1–8 December 2011), followed by a strong increase of daily averages from 300 to 1200 pptv at the beginning of Period III. (~~9–11~~ 9–22 December 2011) (Fig. 1c). After that NO_x mixing ra-

tios gradually dropped over 10 days (Period III.–IV.) to median concentrations of ~120 pptv, slightly lower than observed in late November (Fig. 1c, Table 2). During Period III. ~~(9–22 December 2011)~~ the median concentration of NO_x at 1.0 m was 451 pptv, about 2.5 times that during the same time period in 2009, but similar thereafter (Fig. 1c, Table 2).

The NO_x fluxes, F_{NO_x}, between 0.01 and 1.0 m were mostly emissions from the snow surface, with a median of 1.6×10^{13} molecule $m^{-2} s^{-1}$. Median values of F_{NO_x} at midnight and at noon were 0.4 and 2.9 $\times 10^{13}$ molecule $m^{-2} s^{-1}$, respectively (Table 1). During Period III. F_{NO_x} showed an increase by a factor 3, approximately around the same time when atmospheric mixing ratios of NO_x increased (Fig. 1d, Table 2). The median flux of NO_x during ~~9–22 December 2011~~ Period III. reached 3.1×10^{13} molecule $m^{-2} s^{-1}$, almost 5 times the season median from 2009–2010. During ~~23 December to 12 January~~ (Period IV. (23 December 2011–12 January 2012) the median flux of NO_x in 2011–2012 was about twice that observed in 2009–2010 (Table 2). Potential causes of significant variability in mixing ratios and flux on seasonal time scales are discussed in Sect. 3.5.

3.2 The lower atmosphere-firn air profile

On 9 January 2012 a total of 12 vertical atmospheric profiles of NO_x mixing ratios were measured between 11:30 and 23:30 LT. The lower 100 m of the atmosphere appear well mixed throughout the afternoon, with modelled mixing heights h_z of 200–550 m and observed turbulent diffusion coefficients of heat K_h of $\sim 0.1\, m^2\, s^{-1}$ (Fig. 2). However, in the late afternoon K_h values decreased gradually over a few hours to reach in the evening levels half those during the day thereby giving evidence of strongly reduced vertical mixing. Furthermore, around 18:30 LT modelled h_z values decreased within minutes from 550 to < 15 m height (Fig. 2a) illustrating the collapse of the convective boundary layer typically observed at Dome C in the early evening during summer (King et al., 2006). At Dome C rapid cooling of the surface in the evening results in a strong shallow surface inversion (e.g. Frey et al., 2013), and is illustrated by a decrease in downward long-wave radiation and a negative heat flux, as observed in the evening of 9 January 2012 (Argentini et al., 2014, Fig.4). It follows that NO_x snow emissions are trapped near the surface, which then leads to a significant increase in NO_x mixing ratios below 15 m height measured almost immediately after collapse of the boundary layer (Fig. 2). During 22:20–22:40 LT a small increase in K_h, due to the nightly increase in wind shear (see Frey et al., 2013), was sufficient to cause upward mixing of NO_x accumulated near the surface to ~ 35 m height (Fig. 2). The

vertical balloon soundings further underline the unique geographical setting of Dome C or other sites of similar latitude on the East Antarctic Plateau where air chemistry is dominated by strong diurnal cycles, both in down-welling solar radiation and atmospheric stability, contrasting South Pole where diurnal changes are absent and changes are more due to synoptic variability (Neff et al., 2008).

A vertical profile of mixing ratios of NO_x and O_3 in firn air was measured on 12 January 2012 between 10:00 and 18:00 LT, for which depths were sampled in random order for 30–60 min each. Mixing ratio maxima of NO and NO_2 were ~ 1 and 4 ppbv, respectively, about one order of magnitude above ambient air levels (Table 1), and occurred at 10–15 cm depth, slightly below the typical e-folding depth of 10 cm of wind pack snow at Dome C (France et al., 2011) (Fig. 3a). NO dropped off quickly with depth, reaching 55 pptv at 85 cm, whereas NO_2 decreased asymptotically approaching ~ 2 ppbv (Fig. 3a). NO_3^- concentrations in snow under the firn air probe did not follow the exponential decrease with depth typically observed at Dome C (e.g. Erbland et al., 2013). The firn air probe was installed onto untouched snow, and only removed after the end of the atmospheric sampling period. Thus contamination due to local activity appears unlikely, but a local anomaly remains a possibility as snow pits 5 m next to the lab shelter showed a similar increase of concentration with depth (data not shown). But NO_3^- values within one e-folding depth were still in the range measured further away (Profiles P1–P3 in Fig. 3a), justifying a discussion of vertical profiles of mixing ratios.

O_3 mixing ratios in firn air were always below ambient air levels, suggesting the snow pack to be an O_3 sink as observed previously for the snowpack on the Greenland ice sheet (Peterson and Honrath, 2001), and showed a significant anti-correlation with NO_2 ($R = -0.84$, $p < 0.001$). This is further evidence for significant release of NO_x by the snow matrix into the interstitial air, which then titrates O_3 through the reaction $NO + O_3 \rightarrow NO_2 + O_2$ (Fig. 3). In particular, the drop of O_3 mixing ratios by >10 ppbv at 45 cm depth was not an outlier since collocated NO_2 mixing ratios were also significantly elevated compared to adjacent snow layers (Fig. 3a). However, no snow NO_3^- measurements were available to further investigate the origin of the NO_2 peak. The observed vertical trends in NO_x suggest that below a few e-folding depths the open pore space of the upper snowpack holds a significant reservoir of NO_2 produced photolytically above, as hypothesized previously (Frey et al., 2013). In contrast, NO disappears at depths devoid of UV irradiance as it reacts with O_3.

3.3　Response to UV irradiance

Changes in surface downwelling UV irradiance lead to a quick response of mixing ratios and speciation of NO_x in ambient and firn air as observed during a partial solar eclipse and during a shading experiment (Fig. 4). The solar eclipse occurred early in the season, on 25 November 2011, and caused a decrease in ambient NO mixing ratios at 1.0 m by about 10 pptv or 10 %, whereas NO_2 mixing ratios did not change significantly (Fig. 4a and b). The NO gas phase source, UV photolysis of NO_2, is reduced during the solar eclipse. But the sink of NO, the fast titration with O_3, is unaffected by the reduction in UV irradiance. During the shading experiment on 11 January 2012 plastic sheets were placed at 1 m above the snow surface, alternating in 30 min intervals between UV-opaque and UV-transparent materials. The impact of blocking incident UV irradiance (wavelengths < 380 nm) on firn air mixing ratios at 10 cm snow depth was up to 300 pptv or 30 % decrease in mixing ratios of NO, whereas mixing ratios of NO_2 increased at the same time by $\sim$ 150 pptv or 5 %, although often not statistically significant (Fig. 4c and d). Similar to the solar eclipse, the behavior of NO_x mixing ratios in firn air is in accordance with a disruption of the fast gas phase interconversion of NO_x species. Decrease of NO and increase of NO_2 mixing ratios are consistent with the suppression of NO_2 photolysis, which is both a NO source and a NO_2 sink.

Most importantly varying incident UV irradiance in the wavelength region of NO_3^- absorption (action spectrum maximum at 320 nm) over half-hourly time scales does not cause a depletion of NO_2 in firn air even though NO_2 is the main product of NO_3^- photolysis in the snowpack. A dampened UV response of NO_2 mixing ratios suggests that the NO_x reservoir present in the open pore space of the upper snow pack discussed above must be large as it is not depleted during 30 min filter changes at the sample pump rates used. One implication is that the impact of changes in incident UV irradiance on the snow source and thus NO_x flux and mixing ratios is only observable on diurnal and seasonal time scales.

3.4　$NO_2 : NO$ ratios, peroxy and halogen radicals

In 2011–2012 the $NO_2 : NO$ ratios at 1.0 m were up to 3 times larger than in 2009–2010 (Table 2). A previous steady-state analysis indicated that high peroxy and possibly halogen radical levels must be present to explain ~~large~~ deviations from the simple Leighton steady-state (Frey et al., 2013). The OPALE campaign provided observations needed to further investigate the $NO_2 : NO$ ratios at Dome C.

During summer 2011–2012 median concentrations of RO_2 radicals at 3 m, thought to consist mainly of HO_2 and CH_3O_2, were 9.9×10^7 molecule cm^{-3} (Kukui et al., 2014).

Figure 5 shows the BrO results, where the apparent vertical amounts at 15° are much larger than those at lower elevations – ~~the AMFs are incorrect, and~~ this shows that the vertical profile of BrO used to calculate AMFs, whereby all the BrO is in the boundary layer, must be incorrect. And interestingly, as at Halley in 2007 (Roscoe et al., 2014), much of the BrO must be in the free troposphere. The average of BrO at the three elevations is about 0.8×10^{13} molecule cm^{-2}, with a slight decrease during the campaign. The average at Halley in 2007 was about 2.5×10^{13} molecule cm^{-2}, so mixing ratios of BrO at Dome C are about a third those at Halley. The Dome C data were not inverted to determine the mixing ratio near the surface, but the changes in slant column with elevation angle are similar to those at Halley in 2007 (Roscoe et al., 2014). ~~So if the Halley inversion results are simply divided by~~ Based on the similarity of relative changes of slant BrO with elevation angles to those of Halley in 2007, and the approximate ratio of the slant columns at Halley in 2007 to those at Dome C of 3~~the Dome C values imply 2 to~~, we decided to divide the Halley inversion results by a factor 3 to arrive at a first estimate for Dome C of 2-3 pptv of BrO near the surface. Higher levels prevailing in the free troposphere possibly originate from a sea ice source in coastal Antarctica (Theys et al., 2011) or from stratospheric descent (Salawitch et al., 2010).

Assuming steady-state the total radical concentration $[OX] = [HO_2] + [RO_2] + 2[XO]$, with XO=BrO, ~~,~~ can be calculated based on observed $NO_2 : NO$ ratios and $J(NO_2)$ (Ridley et al., 2000). Repeating the calculation as described in Frey et al. (2013) for 19 December 2011 to 9 January 2012 yields a median [OX] of 2.2×10^9 molecule cm^{-3} or 116 pptv. ~~Median~~ However, during the same period observations showed a median concentration of 9.9×10^7 molecule cm^{-3} or 5 pptv ~~observed during the same period (Kukui et al., 2014) and~~ of $[RO_2] + [HO_2]$ (Kukui et al., 2014) and approximately 3 pptv of ~~BrO yield~~ BrO, yielding a total radical concentration [OX] of 11 pptv. Hence, ~~the estimated total radical concentration exceeds~~ [OX] deduced from measured $NO_2 : NO$ ratios exceeds available observations by a factor 10.3. ~~To estimate the impact of~~ NO_2 mixing ratios were then corrected for a potential interference ~~by~~ with HO_2NO_2 ~~we corrected the mixing ratios, assuming that additional is measured in the CLD from thermal decomposition, equivalent to 25 % (100 %) of ambient on the order~~, assuming ambient levels of 130 pptv. ~~We then find~~ It is found that the median steady-state estimate of total oxidant concentrations is still a factor 9.6 ~~(3.3) larger than that observed. Thus, only a part of the inconsistency may be~~

explained by the interference with (not measured). larger than the sum of observed radical mixing ratios. Hence, the large $NO_2 : NO$ ratios observed at Dome C are either the result of an unknown measurement bias or of an unidentified mechanism in boundary layer oxidation chemistry. A similar conclusion was reached in companion papers on the OPALE project (e.g. Legrand et al., 2014; Kukui et al., 2014; Savarino et al., 2015).

3.5 Drivers of seasonal NO_x variability

On diurnal time scales NO_x mixing ratios at Dome C are controlled by the interplay between snowpack source strength and atmospheric physical properties, i.e. turbulent diffusion of heat K_h and mixing height h_z of the boundary layer. The median diurnal cycles of NO_x mixing ratios in 2011-12 show with the exception of Period II. (1-8 December) previously described behaviour (Frey et al., 2013), that is a strong increase around 1800 LT to maximum values, which last into the night time hours (Fig. 6a). Night-time peaks of NO_x are plausible if the weakening of snow emissions is offset by a corresponding decrease of the chemical sink of NO_x, i.e. the $NO_2 + OH$ reaction, assuming no significant change in h_z. This is consistent to a first order taking into account that observed OH concentrations (Kukui et al., 2014) and F_{NO_x} vary in a similar way, by up to a factor 5 between local noon and midnight.

During Period III. (9–22 December 2011) noon time values are similar to Period II. but the increase in the evening has a larger amplitude and generally larger mixing ratios prevail during night time (Fig. 6a). Increased NO_x mixing ratios during Period III. are consistent with the observed NO_x emission flux F_{NO_x}, which always peaked at local noon, but also showed during Period III. a strong increase at all times of the day with a near doubling of the noon time median (Fig. 6b). During Period IV. (23 December 2011–2012 January 2012) the diurnal cycles of both NO_x mixing ratios and F_{NO_x} returned to low values and small diurnal amplitudes (Fig. 6a–b).

Below we evaluate potential causes of the unusual variability in NO_x mixing ratios and flux observed on seasonal time scales.

3.5.1 Atmospheric mixing vs. snow source strength

Similar to explaining diurnal NO_x cycles at Dome C the seasonal variability of daily mean NO_x mixing ratios during the first half of December 2011 can be attributed to a combination of changes in F_{NO_x} and h_z (Fig. 1). The strong increase of NO_x around 11 December 2011 falls into a Period when F_{NO_x} almost tripled, while wind speeds slightly decreased and shallow boundary layer heights prevailed (Fig. 1, Table 2). For example, on 12 December 2011 and 13 December 2011 the modelled diurnal ranges of h_z were 3.4–224 m and 3.6–251 m, respectively, while sodar observations yielded 10–150 m and 5–125 m, respectively (Gallée et al., 2015). After 13 December 2011 F_{NO_x} remained at high values, thus, the decrease of NO_x mixing ratios appears to be primarily caused by stronger upward mixing into a larger volume, wind speeds increased and daily h_z maxima grew, exceeding 600 m on 18 December 2011 (Fig. 1). After 23 December 2011 NO_x mixing ratios drop to low levels, due to smaller F_{NO_x} and a deep boundary layer (Fig. 1).

F_{NO_x} depends on atmospheric turbulence (K_h) and concentration difference (ΔNO_x), which in turn is determined by the strength of the photolytic snow pack source at a given K_h (Eq. 1–2). However, the relative importance of K_h and snow pack source strength can vary. For example, during Period IV. (23 December 2011–12 January 2012) the median F_{NO_x} was 1.3×10^{13} molecule $m^{-2} s^{-1}$, about twice that observed during the same period in 2009–2010 (Fig. 6g; Table 2). The inter-seasonal difference can be explained by both, significantly larger atmospheric turbulence and more negative ΔNO_x during all times of the day in 2011–2012 (Fig. 6h and i). Median K_h was 0.08 $m^2 s^{-1}$, double that in 2009–2010, and median ΔNO_x was -51 pptv compared to -32 pptv in 2009–2010 (Table 2).

In contrast, during 2011–2012 the observed intra-seasonal variability of F_{NO_x} is dominated by changes in the snow pack source strength. During Period III. (9–22 December 2011) median K_h values ($\sim 0.05 \, m^2 s^{-1}$) and diurnal cycles were smaller than thereafter (Fig. 6c; Table 2), while ΔNO_x values were among the largest observed so far at Dome C, about three times those during the rest of the season, and therefore primarily caused the tripling of F_{NO_x} (Fig. 6d and i). In section 3.5.2 we'll discuss underlying causes of changes in the strength of the snow source.

Previously, non-linear HO_x-NO_x chemistry and the associated increase in NO_x lifetime were suggested to be an additional factor needed to explain large increases in NO_x mixing ratios observed at South Pole (Davis et al., 2008, and references therein). In order to assess the relevance of this factor at Dome C we apply a simple box model to estimate net NO_x production rates as done previously (Frey et al., 2013). It is assumed that mixing is uniform and instantaneous, that the snow emission flux F_{NO_x} is the main NO_x source and the reaction with the OH radical is the dominant NO_x sink and

$$\frac{d[NO_x]}{dt} \sim \frac{F_{NO_x}}{h_z} - k[NO_2][OH] \qquad (4)$$

where k is the respective reaction rate coefficient. In 2009–10 no OH observations were available at Dome C and average values from South Pole were used instead. In 2009–10 estimated net production rates of

NO_x at night were on the order of $100\,\mathrm{pptv\,h^{-1}}$ and therefore explained the average increase in NO_x from 110 to $300\,\mathrm{pptv}$ observed from 1700 to $1900\,\mathrm{LT}$ (Frey et al., 2013). In 2011–12 the same analysis is repeated using OH measurements available for most of Period IV. (Kukui et al., 2014) as well as h_z calculated with the MAR model (Gallée et al., 2015). Resulting night time values of net NO_x production rates are with about $40\,\mathrm{pptv\,h^{-1}}$ smaller than in 2009-10 but again to a first order consistent with a smaller observed increase in NO_x mixing ratios in the evening hours; i.e. during Period IV. median NO_x increased between 1630 and $1930\,\mathrm{LT}$ from 114 to $242\,\mathrm{pptv}$ ((Fig. 6a,f). The above model is oversimplified as the ~~very~~ likely presence of HO_2NO_2 will modulate the diurnal variability of NO_x sinks and sources with an impact on NO_x lifetime as suggested by Davis et al. (2008). However without any information on the diurnal cycle of HO_2NO_2 at Dome C further modelling is not warranted.

3.5.2 Snow source strength

The NO_x flux observed above polar snow is on the order of 10^{12} to $10^{13}\,\mathrm{molecule\,m^{-2}\,s^{-1}}$ and contributes significantly to the NO_x budget in the polar boundary layer. At the lower end of the range are F_{NO_x} observations at Summit, Greenland (Honrath et al., 2002) and at Neumayer in coastal Antarctica (Jones et al., 2001) with $2.5\times10^{12}\,\mathrm{molecule\,m^{-2}\,s^{-1}}$, whereas on the Antarctic Plateau F_{NO_x} values are up to ten times larger. For example, the average F_{NO_x} at South Pole during 26-30 November 2000 was $3.9\times10^{12}\,\mathrm{molecule\,m^{-2}\,s^{-1}}$ (Oncley et al., 2004), whereas at Dome C observed fluxes are 2-6 times larger, with seasonal averages of 8-$25\times10^{12}\,\mathrm{molecule\,m^{-2}\,s^{-1}}$ (Frey et al., 2013, this work). Due to the uncertainties in the processes leading to NO_x production it had been difficult to explain inter-site differences, e.g. by simply scaling F_{NO_x} with UV irradiance and NO_3^- in the surface snow pack (Davis et al., 2004). Some of the variability in flux values may be due to differences in experimental set up or in the employed flux estimation method (e.g. Davis et al., 2004; Frey et al., 2013). For example, the F_{NO_x} estimates for South Pole are based on measured NO gradients only, inferring NO_x from photochemical equilibrium and using the Bowen ratio method (Oncley et al., 2004), whereas the F_{NO_x} estimates for Dome C are based on observations of both atmospheric nitrogen oxides (NO and NO_2) and the flux-gradient method (Frey et al., 2013).

Model predictions of F_{NO_x} show in general a low bias on the Antarctic Plateau when compared to observations. A first 3-D model study for Antarctica included NO_x snow emissions parameterised as a function of temperature and wind speed to match the observed F_{NO_x} at South Pole (Wang et al., 2007). How-

ever, the model under-predicts NO mixing ratios observed above the wider Antarctic Plateau highlighting that the model lacks detail regarding the processes driving the emission flux (Wang et al., 2007). The first model study to calculate F_{NO_x} based on NO_3^- photolysis in snow, as described in this work, reports 1-$1.5\times10^{12}\,\mathrm{molecule\,m^{-2}\,s^{-1}}$ for South Pole in summer (Wolff et al., 2002), about a factor 4 smaller than the observations by Oncley et al. (2004) and up to 16 times smaller than what is needed to explain rapid increases in NO_x mixing ratios over a few hours (Davis et al., 2008, and references therein). Recent model improvements reduced the mismatch with the South Pole flux observations and included the use of updated absorption cross sections and quantum yield of the NO_3^- ~~ion~~ anion, as well as e-folding depths measured in surface snow on the Antarctic Plateau, and resulted in a factor 3 increase of flux calculated for South Pole (France et al., 2011). In light of major remaining uncertainties, which include the spatial variability of NO_3^- in snow and the quantum yield of NO_3^- photolysis (Frey et al., 2013), we discuss below the variability of F_{NO_x} observed at Dome C.

A number of factors may contribute to changes in snow source strength of NO_x. One possibility to explain increases in F_{NO_x} is that the NO_2 reservoir in the open pore space of the upper snowpack discussed above may undergo venting upon changes in atmospheric pressure. However, no statistically significant relationship between F_{NO_x} and atmospheric pressure is found (data not shown). The main cause of large F_{NO_x} values appears rather to be related to changes in snow production rates of NO_x from NO_3^- photolysis, which depend on the NO_3^- photolysis rate coefficient $J_{NO_3^-}$ and the NO_3^- concentration in the photic zone of the snow pack (Eq. 3).

Trends in down-welling UV irradiance due to stratospheric O_3 depletion were suggested previously to drive $J_{NO_3^-}$ and therefore F_{NO_x} and the associated increase in net production of surface O_3 observed at South Pole in summer since the 1990's (Jones and Wolff, 2003). At Dome C the observed increase in F_{NO_x} and strongly negative ΔNO_x values coincided with a period when total column O_3 declined from > 300 to about $250\,\mathrm{DU}$ (Fig. 7a and c). During Period III. ~~(9–22 December 2011)~~ the median column O_3 was about 8% lower than during the time periods before and after (Table 2). However, associated changes in $J_{NO_3^-}$ on the order of $\sim 10\%$ are too small to account alone for the observed tripling in F_{NO_x} (Fig. 6e; Table 2).

Instead changes in F_{NO_x} can be linked to the temporal variability of NO_3^- present in the snow skin layer. During the end of Period II. and beginning of Period III. skin layer NO_3^- concentrations were up to two times larger than before and after (Fig. 7b). F_{NO_x} is high during the

end of Period II. and beginning of Period III., however drops off one week after the decrease of nitrate concentrations in surface snow (Fig. 7c). To confirm the link between NO_x emissions and NO_3^- in snow F_{NO_2} values were modelled (Eq. 3) based on observed $J_{NO_3^-}$, daily sampling of skin layer NO_3^- and two depth profiles, at 100 m (P1) and 5 km (P2) distance from the lab shelter, in order to account for spatial and temporal variability of NO_3^- in snow. Modelled F_{NO_2} capture some of the temporal trends in observational estimates of F_{NO_x} confirming the link with $J_{NO_3^-}$ and NO_3^- concentrations (Fig. 7c). However, median ratios of observed F_{NO_x} and modelled F_{NO_2} values are 30–50 during Period III. and 15–30 during Period IV. (Fig. 7c).

Disagreement between model and observations was previously attributed to ~~uncertainties in the~~ the poorly constrained quantum yield of NO_3^- photolysis in natural snow (Frey et al., 2013). The model employed here uses a constant quantum yield, i.e. its value at the mean ambient temperature at Dome C ($-30\,^\circ$C) of 0.0019 (Chu and Anastasio, 2003). However, quantum yield may vary with time, as the same lab study reports a positive relationship between quantum yield and temperature (Chu and Anastasio, 2003). Comparison of time periods before and after 18 December 2011 shows an increase of mean air temperature from $-34.2\,^\circ$C to $-27.7\,^\circ$C and a decrease of its mean diurnal amplitude from 13 to 9.7 K (Fig. 1a). However, observations of F_{NO_x} showed behaviour opposite to that expected from a temperature driven quantum yield, i.e. F_{NO_x} values decreased as air temperature increased (Fig. 1a and d). Yet, the large diurnal amplitude of air temperature at Dome C could explain diurnal changes of F_{NO_x} by a factor 1.5–1.75. ~~The temperature effect is however~~ However, contributions from the temperature effect are small when compared to the up to 20-fold change between night and day observed in F_{NO_x}~~, which is driven by actinic flux~~. A recent lab study found that the quantum yield of photolytic loss of NO_3^- from snow samples collected at Dome C decreased from 0.44 to 0.003 within what corresponds to a few days of UV exposure in Antarctica (Meusinger et al., 2014). The authors argue that the observed decrease in quantum yield is due to NO_3^- being made of a photolabile and a photo-stable fraction, confirming a previous hypothesis that the range of quantum yields reflects the location of NO_3^- within the snow grain and therefore availability to photolysis (Davis et al., 2008; Frey et al., 2013). Thus, the F_{NO_x} values observed at Dome C fall well within the range of predictions based on quantum yield values measured in snow samples from the same site, which exceed that used in the current model by a factor 2–200. A systematic decrease in quantum yield due to depletion of photo-labile NO_3^- in surface snow may have contributed to the observed decrease in F_{NO_x}

after 22 December 2011. However, a lack of information on snow grain morphology or NO_3^- location within the snow grain limits further exploration of the impact of a time variable quantum yield on F_{NO_x}. It should be noted that during 2009–2010 large skin layer NO_3^- values did not result in F_{NO_x} values comparable to those in 2011–2012 which may be due to a different partitioning between photo-labile and photo-stable NO_3^- in surface snow (Fig. 7b and c; Table 2).

The consequences of large NO_x fluxes consist not only in contributing to high NO_x mixing ratios but also in influencing local O_3 production, as suggested by significantly higher surface O_3 mixing ratios (> 30 ppbv) during 9–22 December in 2011–2012 (Period III.) compared to 25 ppbv in 2009–2010 (Fig. 7d).

4 Conclusions

Measurements of NO_x mixing ratios and flux carried out as part of the OPALE campaign at Dome C in 2011–2012 allowed to extend the existing data set from a previous campaign in 2009–2010.

Vertical profiles of the lower 100 m of the atmosphere confirm that at Dome C large diurnal cycles in solar irradiance and a sudden collapse of the atmospheric boundary layer in the early evening control the variability of NO_x mixing ratios and flux. In contrast, at South Pole diurnal cycles are absent and changes more due to synoptic variability (Neff et al., 2008). Understanding atmospheric composition and air-snow interactions in inner Antarctica requires studies at both sites as they together encompass the spectrum of diurnal variability expected across the East Antarctic Plateau (King et al., 2006; Frey et al., 2013). Large mixing ratios of NO_x at Dome C arise from a combination of several factors: continuous sunlight, large NO_x emissions from surface snow and shallow mixing depths after the evening collapse of the convective boundary layer. Unlike at South Pole it is not necessary to invoke non-linear HO_x-NO_x chemistry to explain increases in NO_x mixing ratios. However, uncertainties remain regarding atmospheric levels of HO_2NO_2 and its impact on NO_x life time being a temporary NO_x reservoir. ~~Understanding atmospheric composition and air-snow interactions in inner Antarctica requires studies at both sites as they together encompass the spectrum of diurnal variability expected across the East Antarctic Plateau (King et al., 2006; Frey et al., 2013).~~

Firn air profiles suggest that the upper snow pack at Dome C is an O_3 sink and holds below a few e-folding depths a significant reservoir of NO_2 produced photolytically above, whereas NO disappears at depths devoid of UV as it reacts with O_3. Shading experiments showed that the presence of such a NO_2 reservoir dampens the

response of NO_x mixing ratios above or within the snow-pack due to changes in down-welling UV irradiance on hourly time scales. Thus, systematic changes in NO_x mixing ratios and flux due to the impact of UV on the snow source are only observable on diurnal and seasonal time scales.

First-time observations of BrO at Dome C sug-gest ~~2–3~~ that mixing ratios of BrO near the ground ~~, with higher levels in the free troposphere similar to Halley, possibly originating from a sea ice source in coastal Antarctica (Theys et al., 2011) or from stratospheric descent (Salawitch et al., 2010)~~ are low certainly less than 5 pptv. Assuming steady-state observed mixing ratios of BrO and RO_2 radicals are about a factor ten too low to explain the $NO_2 : NO$ ratios measured in ambient air. ~~The likely presence~~ A potential interference of HO_2NO_2 ~~at Dome C (not measured) may cause an overestimate of~~ with ~~the detection method employed and explain a~~ with the NO_2 measurements explains only a small part of this inconsistency. Hence, the large $NO_2 : NO$ ratios observed at Dome C are either the result of an unknown measurement bias or of a yet unidentified mechanism in boundary layer oxidation chemistry as similarly concluded in OPALE companion papers (e.g. Legrand et al., 2014; Kukui et al., 2014; Savarino et al., 2015).

During 2011–2012 NO_x mixing ratios and flux were larger than in 2009–2010 consistent with also larger surface O_3 mixing ratios resulting from increased net O_3 production. Large NO_x mixing ratios and significant variability during December 2011 were attributed to a combination of changes in mixing height and NO_x snow emission flux F_{NO_x}. Trends in F_{NO_x} were found to be controlled by atmospheric turbulence and the strength of the photolytic snowpack source, of which the relative importance may vary in time. Larger median F_{NO_x} values in 2011–2012 than those during the same period in 2009–2010 can be explained by both, significantly larger atmospheric turbulence and a slightly stronger snowpack source. However, the tripling of F_{NO_x} in December 2011 was largely due to changes in snow pack source strength driven primarily by changes in NO_3^- concentrations in the snow skin layer, and only to a secondary order by the decrease of total column O_3 and the associated increase in NO_3^- photolysis rates. Median ratios of observed F_{NO_x} and modelled F_{NO_2} values ranged from 15 to 50 using the quantum yield of NO_3^- photolysis reported by Chu and Anastasio (2003). Model predictions based on quantum yield values measured in a recent lab study on Dome C snow samples (Meusinger et al., 2014) yield 2–200 fold larger F_{NO_2} values encompassing observed F_{NO_x}. In particular, a decrease in quantum yield due to depletion of photo-labile

NO_3^- in surface snow may have contributed to the observed decrease in F_{NO_x} after 22 December 2011. Yet in 2009–2010 large skin layer NO_3^- values did not result in elevated F_{NO_x} values as seen in 2011–2012 possibly due to different partitioning of NO_3^- between a photo-labile and photo-stable fraction.

In summary the seasonal variability of NO_x snow emissions important to understand atmospheric composition above the East Antarctic Plateau depends not only on atmospheric mixing but also critically on NO_3^- concentration and availability to photolysis in surface snow, as well as incident UV irradiance. However, the boundary layer chemistry of reactive nitrogen is not fully understood yet. Future studies on the Antarctic Plateau need to reduce uncertainties in NO_2 and HONO measurements, obtain also observations of HO_2NO_2 and assess how quantum yield of NO_3^- photolysis in snow varies as a function of snow chemical and physical properties. This is important to be able to close the mass budget of reactive nitrogen species between atmosphere and snow above Antarctica.

References

Anderson, P. S. and Neff, W. D.: Boundary layer physics over snow and ice, Atmos. Chem. Phys., 8, 3563–3582, doi:10.5194/acp-8-3563-2008, 2008.

Argentini, S., Petenko, I., Viola, A., Mastrantonio, G., Pietroni, I., Casasanta, G., Aristidi, E., and Genthon, C.: The surface layer observed by a high-resolution sodar at DOME C, Antarctica, Annals of Geophysics, 56, 1–10, doi:10.4401/ag-6347, 2014.

Bauguitte, S. J.-B., Bloss, W. J., Evans, M. J., Salmon, R. A., Anderson, P. S., Jones, A. E., Lee, J. D., Saiz-Lopez, A., Roscoe, H. K., Wolff, E. W., and Plane, J. M. C.: Summertime NO_x measurements during the CHABLIS campaign: can source and sink estimates

unravel observed diurnal cycles?, Atmos. Chem. Phys., 12, 989–1002, doi:10.5194/acp-12-989-2012, 2012.

Berhanu, T. A., Savarino, J., Erbland, J., Vicars, W. C., Preunkert, S., Martins, J. F., and Johnson, M. S.: Isotopic effects of nitrate photochemistry in snow: a field study at Dome C, Antarctica, Atmos. Chem. Phys. Disc., 14, 33 045–33 088, doi:10.5194/acpd-14-33045-2014, 2014.

Chu, L. and Anastasio, C.: Quantum yields of hydroxyl radical and nitrogen dioxide from the photolysis of nitrate on ice, J. Phys. Chem. A, 107, 9594–9602, 2003.

Crawford, J. H., Davis, D. D., Chen, G., Buhr, M., Oltmans, S., Weller, R., Mauldin, L., Eisele, F., Shetter, R., Lefer, B., Arimoto, R., and Hogan, A.: Evidence for photochemical production of ozone at the South Pole surface, Geophys. Res. Lett., 28, 3641–3644, 2001.

Davis, D. D., Seelig, J., Huey, G., Crawford, J., Chen, G., Wang, Y. H., Buhr, M., Helmig, D., Neff, W., Blake, D., Arimoto, R., and Eisele, F.: A reassessment of Antarctic plateau reactive nitrogen based on ANTCI 2003 airborne and ground based measurements, Atmos. Environ., 42, 2831–2848, doi:10.1016/j.atmosenv.2007.07.039, 2008.

Davis, D. D., Chen, G., Buhr, M., Crawford, J., Lenschow, D., Lefer, B., Shetter, R., Eisele, F., Mauldin, L., and Hogan, A.: South Pole NO_x chemistry : an assessment of factors controlling variability and absolute levels, Atmos. Environ., 38(32), 5275–5388, doi:10.1016/j.atmosenv.2004.04.039, 2004.

Erbland, J., Vicars, W. C., Savarino, J., Morin, S., Frey, M. M., Frosini, D., Vince, E., and Martins, J. M. F.: Air–snow transfer of nitrate on the East Antarctic Plateau – Part 1: Isotopic evidence for a photolytically driven dynamic equilibrium in summer, Atmos. Chem. Phys., 13, 6403–6419, doi:10.5194/acp-13-6403-2013, 2013.

Fisher, F. N., King, M. D., and Lee-Taylor, J.: Extinction of UV-visible radiation in wet midlatitude (maritime) snow: Implications for increased NO_x emission, J. Geophys. Res., 110, doi:10.1029/2005JD005963, 2005.

France, J. L., King, M. D., and Lee-Taylor, J.: The importance of considering depth-resolved photochemistry in snow: a radiative-transfer study of NO_2 and OH production in Ny-Alesund (Svalbard) snowpacks, J. Glaciol., 56, 655–663, 2010.

France, J. L., King, M. D., Frey, M. M., Erbland, J., Picard, G., Preunkert, S., MacArthur, A., and Savarino, J.: Snow optical properties at Dome C (Concordia), Antarctica; implications for snow emissions and snow chemistry of reactive nitrogen, Atmos. Chem. Phys., 11, 9787–9801, doi:10.5194/acp-11-9787-2011, 2011.

Frey, M. M., Stewart, R. W., McConnell, J. R., and Bales, R. C.: Atmospheric hydroperoxides in West Antarctica: links to stratospheric ozone and atmospheric oxidation capacity, J. Geophys. Res., 110, D23301, doi:10.1029/2005JD006110, 2005.

Frey, M. M., Hutterli, M. A., Chen, G., Sjostedt, S. J., Burkhart, J. F., Friel, D. K., and Bales, R. C.: Contrasting atmospheric boundary layer chemistry of methylhydroperoxide (CH_3OOH) and hydrogen peroxide (H_2O_2) above polar snow, Atmos. Chem. Phys., 9, 3261–3276, doi:10.5194/acp-9-3261-2009, 2009.

Frey, M. M., Savarino, J., Morin, S., Erbland, J., and Martins, J. M. F.: Photolysis imprint in the nitrate stable isotope signal in snow and atmosphere of East Antarctica and implications for reactive nitrogen cycling, Atmos. Chem. Phys., 9, 8681–8696, doi:10.5194/acp-9-8681-2009, 2009b.

Frey, M. M., Brough, N., France, J. L., Anderson, P. S., Traulle, O., King, M. D., Jones, A. E., Wolff, E. W., and Savarino, J.: The diurnal variability of atmospheric nitrogen oxides (NO and NO_2) above the Antarctic Plateau driven by atmospheric stability and snow emissions, Atmos. Chem. Phys., 13, 3045–3062, doi:10.5194/acp-13-3045-2013, 2013.

Gallée, H. and Gorodetskaya, I.: Validation of a limited area model over Dome C, Antarctic Plateau, during winter, Clim. Dynam., 34, 61–72, doi:10.1007/s00382-008-0499-y, 2010.

Gallée, H., Preunkert, S., Argentini, S., Frey, M. M., Genthon, C., Jourdain, B., Pietroni, I., Casasanta, G., Barral, H., Vignon, E., Amory, C., and Legrand, M.: Characterization of the boundary layer at Dome C (East Antarctica) during the OPALE summer campaign, Atmos. Chem. Phys., 15, 6225–6236, doi:10.5194/acp-15-6225-2015, 2015.

Honrath, R. E., Peterson, M. C., Dziobak, M. P., Dibb, J., Arsenault, M. A., and Green, S. A.: Release of NO_x from sunlight-irradiated midlatitude snow, Geophys. Res. Lett., 27, 2237–2240, 2000a.

Honrath, R. E., Guo, S., Peterson, M. C., Dziobak, M. P., Dibb, J. E., and Arsenault, M. A.: Photochemical production of gas phase NO_x from ice crystal NO_3^-, J. Geophys. Res., 105, 24183–24190, 2000b.

Honrath, R., Lu, Y., Peterson, M., Dibb, J., Arsenault, M., Cullen, N., and Steffen, K.: Vertical fluxes of NO_x, HONO, and HNO_3 above the snowpack at Summit, Greenland, Atmos. Environ., 36, 2629–2640, doi:10.1016/S1352-2310(02)00132-2, 2002.

Jacobson, M. Z.: Fundamentals of Atmospheric Modeling, Cambridge University Press, Cambridge, UK, 1999.

Jones, A. E. and Wolff, E. W.: An analysis of the oxidation potential of the South Pole boundary layer and the influence of stratospheric ozone depletion, J. Geophys. Res., 108, doi:10.1029/2003JD003379, 2003.

Jones, A. E., Weller, R., Anderson, P. S., Jacobi, H. W., Wolff, E. W., Schrems, O., and Miller, H.: Measurements of NO_x emissions from the Antarctic snow pack, Geophys. Res. Lett., 28, 1499–1502, 2001.

Kaimal, J. and Finnigan, J. J.: Atmospheric Boundary Layer Flows, Oxford University Press, Oxford, UK, 1994.

King, J. C., Argentini, S. A., and Anderson, P. S.: Contrasts between the summertime surface energy balance and boundary layer structure at Dome C and Halley stations, Antarctica, J. Geophys. Res., 111, D02105, doi:10.1029/2005JD006130, 2006.

Kukui, A., Legrand, M., Preunkert, S., Frey, M. M., Loisil, R., Gil Roca, J., Jourdain, B., King, M. D., France, J. L., and Ancellet, G.: Measurements of OH and RO_2 radicals at Dome C, East Antarctica, Atmos. Chem. Phys., 14, 12373–12392, doi:10.5194/acp-14-12373-2014, 2014.

Lee-Taylor, J. and Madronich, S.: Calculation of actinic fluxes with a coupled atmosphere-snow radiative transfer model, J. Geophys. Res., 107, 4796, doi:10.1029/2002JD002084, 2002.

Legrand, M., Preunkert, S., Jourdain, B., Gallée, H., Goutail, F., Weller, R., and Savarino, J.: Year-round record of surface ozone at coastal (Dumont d'Urville) and inland (Concordia) sites in East Antarctica, J. Geophys. Res., 114, D20306, doi:10.1029/2008JD011667, 2009.

Legrand, M., Preunkert, S., Frey, M., Bartels-Rausch, Th., Kukui, A., King, M. D., Savarino, J., Kerbrat, M., and Jourdain, B.: Large mixing ratios of atmospheric nitrous acid (HONO) at Concordia (East Antarctic Plateau) in summer: a strong source from surface snow?, Atmos. Chem. Phys., 14, 9963–9976, doi:10.5194/acp-14-9963-2014, 2014.

Lenschow, D. H.: Micrometeorological techniques for measuring biosphere–atmosphere trace gas exchange, in: Biogenic Trace Gases: Measuring Emissions from Soil and Water, edited by: Matson, P. A. and Harriss, R. C., Blackwell Science, London, 126–163, 1995.

Mayer, B. and Kylling, A.: Technical note: The libRadtran software package for radiative transfer calculations – description and examples of use, Atmos. Chem. Phys., 5, 1855–1877, doi:10.5194/acp-5-1855-2005, 2005.

Meusinger, C., Berhanu, T. A., Erbland, J., Savarino, J., and Johnson, M. S.: Laboratory study of nitrate photolysis in Antarctic snow. I. Observed quantum yield, domain of photolysis, and secondary chemistry, J. Chem. Phys., 140, 244305, doi:10.1063/1.4882898, 2014.

Neff, W., Helmig, D., Grachev, A., and Davis, D.: A study of boundary layer behavior associated with high NO concentrations at the South Pole using a minisodar, tethered balloons and sonic anemometer, Atmos. Environ., 42, 2762–2779, doi:10.1016/j.atmosenv.2007.01.033, 2008.

Oncley, S. P., Buhr, M., Lenschow, D. H., Davis, D., and Semmer, S. R.: Observations of summertime NO fluxes and boundary-layer height at the South Pole during IS-CAT 2000 using scalar similarity, Atmos. Environ., 38(32), 5389–5398, doi:10.1016/j.atmosenv.2004.05.053, 2004.

Peterson, M. C. and Honrath, R. E.: Observations of rapid photochemical destruction of ozone in snowpack interstitial air, Geophys. Res. Lett., 28, 511–514, 2001.

Preunkert, S., Ancellet, G., Legrand, M., Kukui, A., Kerbrat, M., Sarda-Estève, R., Gros, V., and Jourdain, B.: Oxidant Production over Antarctic Land and its Export (OPALE) project: an overview of the 2010–2011 summer campaign, J. Geophys. Res., 117, doi:10.1029/2011JD017145, 2012.

Ridley, B., Walega, J., Montzka, D., Grahek, F., Atlas, E., Flocke, F., Stroud, V., Deary, J., Gallant, A., Boudries, H., Bottenheim, J., Anlauf, K., Worthy, D., Sumner, A., Splawn, B., and Shepson, P.: Is the Arctic surface layer a source and sink of NOx in winter/spring?, J. Atmos. Chem., 36, 1–22, doi:10.1023/A:1006301029874, 2000.

Roscoe, H., Brough, N., Jones, A., Wittrock, F., Richter, A., Roozendael, M. V., and Hendrick, F.: Characterisation of vertical BrO distribution during events of enhanced tropospheric BrO in Antarctica, from combined remote and

in-situ measurements, J. Quant. Spectrosc. Rad. Trans., 138, 70–81, doi:10.1016/j.jqsrt.2014.01.026, 2014.

Salawitch, R. J., Canty, T., Kurosu, T., Chance, K., Liang, Q., da Silva, A., Pawson, S., Nielsen, J. E., Rodriguez, J. M., Bhartia, P. K., Liu, X., Huey, L. G., Liao, J., Stickel, R. E., Tanner, D. J., Dibb, J. E., Simpson, W. R., Donohoue, D., Weinheimer, A., Flocke, F., Knapp, D., Montzka, D., Neuman, J. A., Nowak, J. B., Ryerson, T. B., Oltmans, S., Blake, D. R., Atlas, E. L., Kinnison, D. E., Tilmes, S., Pan, L. L., Hendrick, F., Van Roozendael, M., Kreher, K., Johnston, P. V., Gao, R. S., Johnson, B., Bui, T. P., Chen, G., Pierce, R. B., Crawford, J. H., and Jacob, D. J.: A new interpretation of total column BrO during Arctic spring, Geophys. Res. Lett., 37, doi:10.1029/2010GL043798, 2010.

Savarino, J., Vicars, W. C., Legrand, M., Preunkert, S., Jourdain, B., Frey, M. M., Kukui, A., Gil and Roca, J.: Oxygen isotope mass balance of atmospheric nitrate at Dome C, East Antarctica, during the OPALE campaign, Atmos. Chem. Phys. Disc., submitted, 2015.

Simpson, W. R., King, M. D., Beine, H. J., Honrath, R. E., and Zhou, X.: Radiation-transfer modeling of snow-pack photochemical processes during ALERT 2000, Atmos. Environ., 36, 2663–2670, 2002.

Slusher, D. L., Neff, W. D., Kim, S., Huey, L. G., Wang, Y., Zeng, T., Tanner, D. J., Blake, D. R., Beyersdorf, A., Lefer, B. L., Crawford, J. H., Eisele, F. L., Mauldin, R. L., Kosciuch, E., Buhr, M. P., Wallace, H. W., and Davis, D. D.: Atmospheric chemistry results from the ANTCI 2005 Antarctic plateau airborne study, J. Geophys. Res., 115, D07304, doi:10.1029/2009JD012605, 2010.

Stull, R. B.: An Introduction to Boundary Layer Meteorology, Kluwer Academic Publishers, Dordbrecht/Boston/London, 1988.

Theys, N., Van Roozendael, M., Hendrick, F., Yang, X., De Smedt, I., Richter, A., Begoin, M., Errera, Q., Johnston, P. V., Kreher, K., and De Mazière, M.: Global observations of tropospheric BrO columns using GOME-2 satellite data, Atmos. Chem. Phys., 11, 1791–1811, doi:10.5194/acp-11-1791-2011, 2011.

Van Dam, B., Helmig, D., Neff, W., and Kramer, L.: Evaluation of Boundary Layer Depth Estimates at Summit Station, Greenland, J. Appl. Meteor. Climatol., 52, 2356–2362, doi:10.1175/JAMC-D-13-055.1, 2013.

Van Dijk, A., Moen, A., and De Bruin, H.: The principles of surface flux physics: theory, practice and description of the ECPACK library, Internal Report 2004/1, Meteorology and Air Quality Group, Wageningen University, Wageningen, the Netherlands, 2006.

Wang, Y. H., Choi, J., Zeng, T., Davis, D., Buhr, M., Huey, G., and Neff, W.: Assessing the photochemical impact of snow NO_x emissions over Antarctica during ANTCI 2003, Atmos. Environ., 41, 3944–3958, doi:10.1016/j.atmosenv.2007.01.056, 2007.

Wolff, E. W., Jones, A. E., Martin, T. J., and Grenfell, T. C.: Modelling photochemical NO_x production and nitrate loss in the upper snowpack of Antarctica, Geophys. Res. Lett., 29(20), doi:10.1029/2002GL015823, 2002.

Table 1. NO_x mixing ratios and flux at Dome C during 23 November 2011–12 January 2012.

Parameter	z, m	mean $\pm 1\sigma$	median	t_{total}, days[a]
NO, pptv	-0.1[b]	1097 ± 795	879	2.9
	0.01	121 ± 102	94	18.6
	1.0	98 ± 80	77	24.4
	4.0	93 ± 68	78	13.7
NO_2, pptv	-0.1[b]	4145 ± 2667	2990	2.6
	0.01	328 ± 340	222	17.6
	1.0	211 ± 247	137	23.2
	4.0	210 ± 199	159	12.8
NO_x, pptv	-0.1[b]	5144 ± 3271	3837	2.6
	0.01	447 ± 432	319	17.5
	1.0	306 ± 316	213	23.2
	4.0	302 ± 259	241	12.8
$F-NO_x \times 10^{13}$ molecule $m^{-2} s^{-1}$[c]	0.01–1.0	2.5 ± 8.2	1.6	17.4
$F-NO_x \times 10^{13}$ molecule $m^{-2} s^{-1}$, local noon	0.01–1.0	5.0 ± 8.2	2.9	1.1
$F-NO_x \times 10^{13}$ molecule $m^{-2} s^{-1}$, local midnight	0.01–1.0	0.3 ± 1.6	0.4	0.2

[a] Total sample time estimated as the sum of all 1 min intervals.
[b] Firn air sampled during 20–22 December 2011, 1–5 January 2012 and 10–14 January 2012.
[c] 1 December 2011–12 January 2012.

33

Table 2. Seasonal evolution of median NO_x mixing ratios and flux along with relevant environmental parameters at Dome C in summer 2011–2012 (time periods I.–IV. highlighted in Fig. 1 and 7) and comparison to summer 2009–2010 (from Frey et al., 2013).

| Parameter	I. 23 Nov 2011– 30 Nov 2011	II. 1 Dec 2011– 8 Dec 2011	III. 9 Dec 2011– 22 Dec 2011	IV. 23 Dec 2011– 12 Jan 2012	9 Dec 2009– 22 Dec 2009	23 Dec 2009– 12 Jan 2010
NO_x (pptv)[a]	180	324	451	122	183	145
$F-NO_x \times 10^{13}$ (molecule $m^{-2} s^{-1}$)[b]	–	0.94	3.10	1.30	–	0.66
ΔNO_x (pptv)[b]	–	-63	−153	−51	–	−32
$NO_2 : NO$[a]	1.3	1.5	2.8	2.0	1.1	0.60
T_{air} (°C)	−34.5	−34.5	−31.0	−27.4	−31.5	−30.9
wind speed ($m s^{-1}$)	6.3	3.0	2.5	3.8	2.4	2.2
K_h ($m^2 s^{-1}$)	–	0.046	0.049	0.080	–	0.043
h_z (m) [c]	–	19	20	36	6–59	18–25
$J_{NO_3^-} \times 10^{-8}$ (s^{-1})	–	–	2.93	2.68	–	–
SZA (°)	69.7	68.1	67.6	67.9	67.6	67.9
column O_3 (DU)	301	294	272	297	311	309
NO_3^- skin layer (ng g^{-1})[d]	513	764	1090	439	866	1212
O_3 (ppbv)	34.2	35.7	31.9	21.1	24.6	22.6

[a] At 1 m above the snow surface.
[b] Based on concentrations at 1.0 and 0.01 m above the snow surface.
[c] Model estimates.
[d] From daily sampling of the top 0.5 cm of snow.
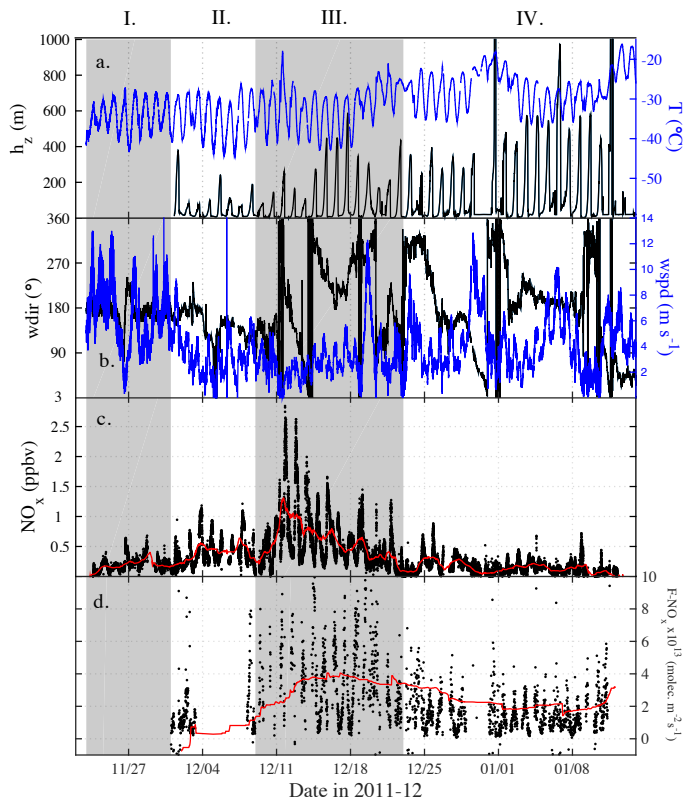
Figure 1. Meteorology and NO_x observations at Dome C in summer 2011–2012 (highlighted periods I.–IV. as referred to in text and Table 2): **(a)** air temperature (T) at 1.6 m and modeled mixing height (h_z) (Gallée et al., 2015), **(b)** wind speed (wspd) and direction (wdir) at 3.3 m **(c)**, 1 min averages of NO_x mixing ratios at 1 m (red line is 1 day running mean) and **(d)** 10 min averages of observational estimates of NO_x flux (F_{NO_x}) between 0.01 and 1 m (red line is 14 day running mean).
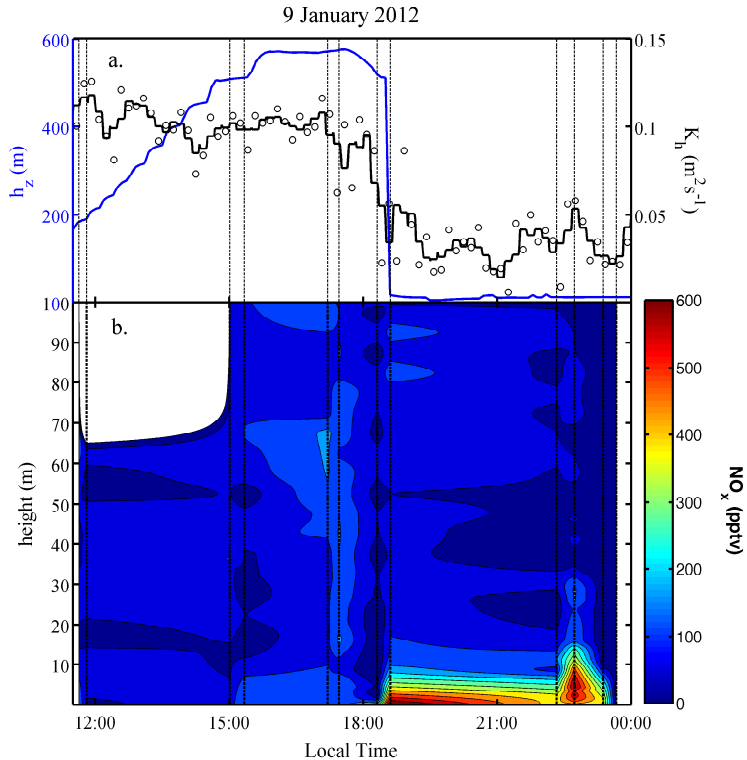
Figure 2. Balloon profiles (vertical dashed lines) from 9 January 2012: **(a)** modelled mixing height h_z (10 min running mean) and observed turbulent diffusion coefficient of heat K_h at 1 m (symbols: 10 min averages; black line: 30 min running mean). **(b)** interpolated vertical profiles of NO_x mixing ratios with contour lines representing 60 pptv intervals. The lower 100 m appear well mixed during the day, while after collapse of the convective boundary layer in the early evening snow emissions of NO_x are trapped near the surface causing a strong increase in mixing ratios near the ground.
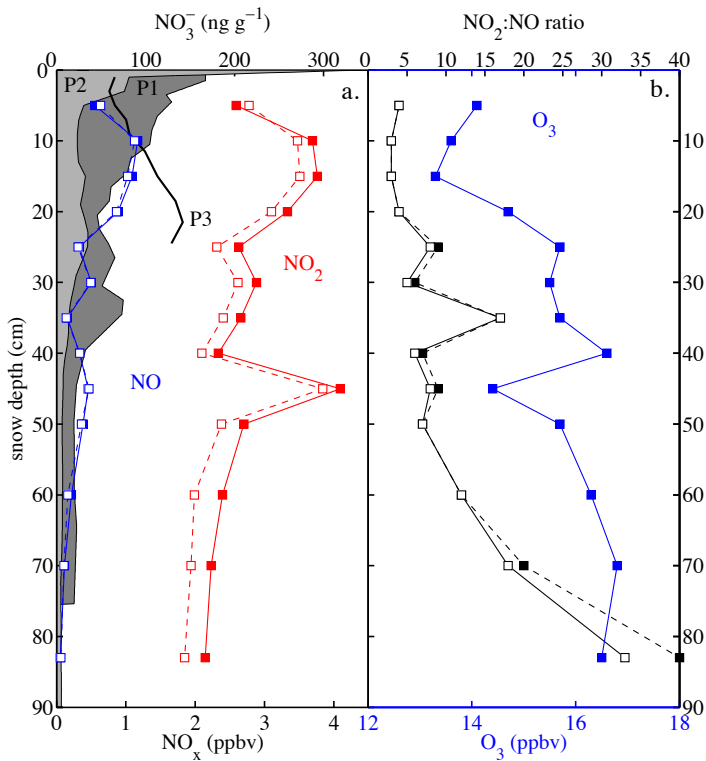
**Figure 3.** Firn air mixing ratios of **(a)** NO_x and **(b)** O_3, observed on 12 January 2012. Symbols represent 30 min averages. Solid and dashed lines are results from 20 m and 50 m long intake lines, respectively. Shown are also NO_3^- concentrations in snow at 100 m (P1) and 5 km (P2) distance from the lab shelter as well as from under the firn probe (P3).
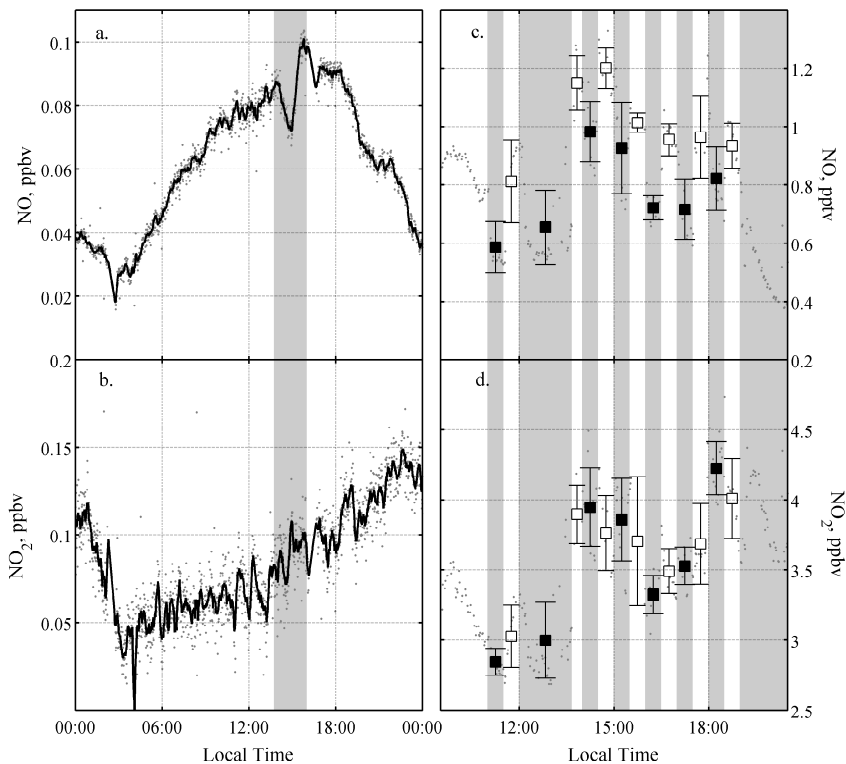
Figure 4. The impact of rapid changes in incident solar radiation on atmospheric NO_x mixing ratios (1 min values). **(a–b)** ambient concentrations at 1 m during a partial solar eclipse on 25 November 2011 (shaded area) with black lines representing the 10 min running mean. **(c–d)** firn air concentrations at 10 cm depth during a shading experiment using UV-filters on 11 January 2012. Square symbols and error bars represent interval averages and standard deviation, respectively. Shaded areas and filled squares indicate time periods when the UV filter was in place.
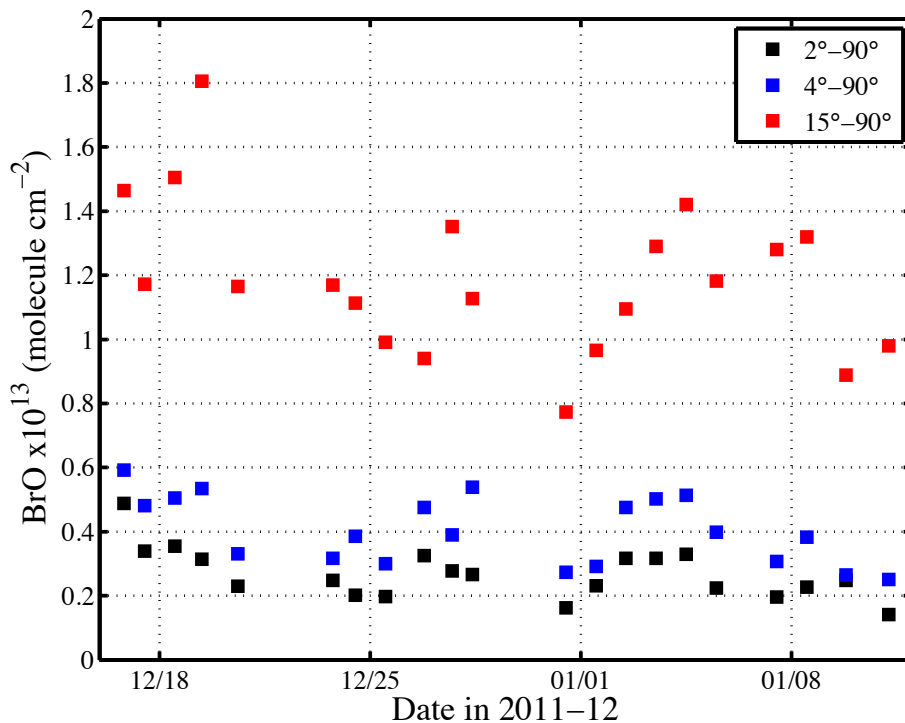
Figure 5. Median daily values of MAX-DOAS BrO vertical amounts from Dome C during sunny days or part-days only, after subtracting zenith amounts (see text). Reference spectrum from near-noon on 18 December 2011 until 6 January 2012, then from near noon on 7 January 2012. The apparently larger vertical amounts at higher elevations show that much of the BrO is in the free troposphere.
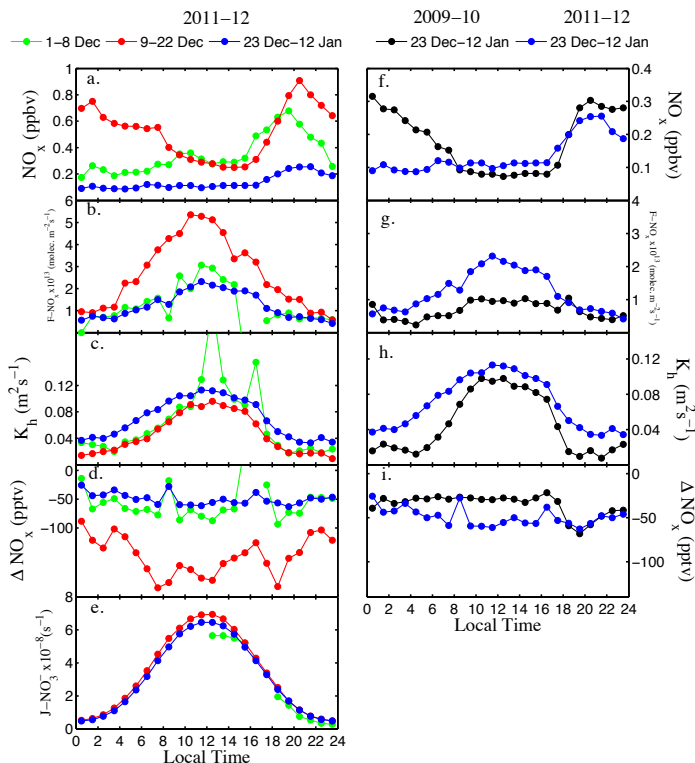
Figure 6. Observed median diurnal cycles during selected intervals in **(a–e)** 2011–2012 (referred to as periods II.–IV. in Table 2, Figs. 1, 7) and **(f–i)** 2009–2010. Shown are **(a, f)** NO_x mixing ratios at $1\,m$, **(b, g)** NO_x flux (F-NO_x) between 0.01 and $1\,m$, **(c, h)** the turbulent diffusion coefficient of heat (K_h) at $1\,m$, **(d, i)** the difference in NO_x mixing ratios (ΔNO_x) between 1.0 and $0.01\,m$, and **(e)** the 2π downwelling nitrate photolysis rate coefficient $(J_{NO_3^-})$. Note comparable observations of $J_{NO_3^-}$ are not available from 2009–2010.
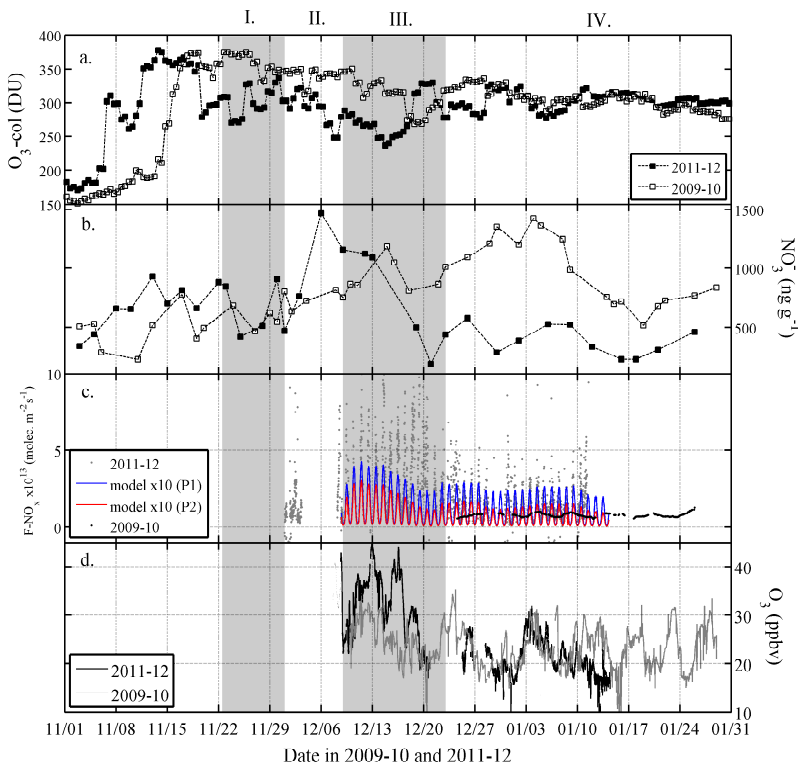
Figure 7. (a) Total column O_3 above Dome C. **(b)** NO_3^- concentrations in the skin layer of surface snow (top 0.5 cm). **(c)** observational estimates of NO_x flux (F_{NO_x}) between 0.01 and 1 m (10 min averages) and modelled F_{NO_2} (multiplied by 10) based on NO_3^- in the skin layer and depth profiles observed at 100 m (P1) and 5 km (P2) distance from the lab shelter (see Fig. 3a); the 1 day running mean of F_{NO_x} during 2009–2010 is shown for comparison (from Frey et al., 2013) **(d)** atmospheric O_3 mixing ratios. Highlighted periods I.–IV. as referred to in text and Table 2.